DISSERTATION

The Pathophysiological Role of Toll-like Receptor 2 Activation in Neutrophil Granulocytes in Patients with Acute Coronary Syndrome with Intact vs. Ruptured Fibrous Cap

Die pathophysiologische Rolle der Toll-like Rezeptor 2 Aktivierung in den neutrophilen Granulozyten in Patienten mit Akutem Koronarsyndrom mit intakter oder rupturierter fibröser Kappe

zur Erlangung des akademischen Grades
Doctor medicinae (Dr. med.)

vorgelegt der Medizinischen Fakultät
Charité – Universitätsmedizin Berlin

von

Denitsa Meteva

Erstbetreuerin: PD Dr. rer. nat. Nicolle Kränkel

Datum der Promotion: 29.11.2024

Table of Contents

List of Tables

List of Figures

List of Abbreviations

ACS	Acute Coronary Syndrome
ANOVA	Analysis of Variance
BL	Blue Laser
BMI	Body Mass Index
CAD	Coronary Artery Disease
CD	Cluster of Differentiation
CK	Creatinine Kinase
CL	Culprit Lesion
CXCR4	Chemokine Receptor Type 4
DAPI	4′,6-diaminophenylindole
ECD	Endothelial cell desquamation
EDTA	Ethylenediaminetetraacetic Acid
EGM	Endothelial Cell Growth Medium
FBS	Fetal Bovine Serum
FC	Fibrous Cap
FCS	Fetal Calf Serum
FSC-H	Forward Scatter Height
FSC-W	Forward Scatter Width
HA	Hyaluronic Acid
HAECs	Human Aortic Endothelial Cells
HDL	High-density Lipoprotein
HEPES	4-(2-hydroxyethyl)-1-piperazineethane Sulfonic Acid
hsCRP	High sensitive C-reactive Protein
HYAL2	Hyaluronidase 2
IFC-ACS	Acute Coronary Syndrome with intact Fibrous Cap
IQR	Interquartile Range
LDL	Low-density Lipoprotein
LOC	Local
LVEF	Left Ventricular Ejection Fraction
MFI	Median Fluorescence Intensity
MLA	Minimum Lumen Area

MMP9	Matrix Metalloproteinase 9
n	Number
NETs	Neutrophil Extracellular Traps
NGAL	Neutrophil-gelatinase Associated Lipocalin
NSTEMI	Non ST-segment elevation myocardial infarction
OCT	Optical Coherence Tomography
OPTI-MEM	Optimized Minimal Essential Medium
oxLDL	Oxidized Low-density Lipoprotein
Pam3CSK4	Pam3CysSerLys4
PCI	Percutaneous Coronary Intervention
PI	Propidium Iodide
PMNs	Polymorphonuclear Neutrophils
RFC-ACS	Acute Coronary Syndrome with ruptured Fibrous Cap
RPMI 1640	Roswell Park Memorial Institute 1640 Medium
SD	Standard Deviation
SMD	Standardized Mean Difference
SSC-H	Side Scatter Height
STEMI	ST-Segment Elevation Myocardial Infarction
SYS	Systemic
TCFA	Thin Cap Fibroatheroma
TLR1	Toll-like Receptor 1
TLR2	Toll-like Receptor 2
TLR4	Toll-like Receptor 4
VEGFR1	Vascular Endothelial Growth Factor Receptor 1
VL	Violet Laser

Zusammenfassung

Nur zwei Drittel der Myokardinfarkte werden durch eine Plaque-Ruptur ausgelöst, während bei ca. einem Drittel der Patienten die fibröse Kappe intakt bleibt und die Thrombogenese durch den Verlust der Endothelzellschicht hervorgerufen wird (1).

Der Mechanismus der Plaque-Ruptur (RFC-ACS) ist durch das Konzept der vulnerablen Plaque mit großem Lipidkern und dünner fibröser Kappe bereits gut charakterisiert(2). Im Gegensatz dazu ist die Pathogenese der Plaque-Erosion (IFC-ACS) nicht vollständig verstanden. Aus Post-mortem--Analysen(3, 4) und aus ersten pathophysiologischen Studien(5, 6) ergeben sich für die Plaque-Erosion Hinweise für spezifische inflammatorische Mechanismen mit Fokus auf die neutrophilen Granulozyten als die ersten Immunzellen und im Verlauf die T-Zellen(7). Mittels optischer Kohärenztomographie (OCT) ist es heutzutage möglich in-vivo die Diagnose der Plaque-Erosion oder –Ruptur zu stellen und damit unterliegende Pathomechanismen in-vivo zu untersuchen. Das Ziel der vorliegenden Arbeit ist es die genaue Rolle der neutrophilen Granulozyten in der Pathophysiologie der Plaque-Erosion und Plaque-Ruptur besser zu charakterisieren.

Es wurden zweiunddreißig Patienten mit Plaque-Erosion zu zweiunddreißig Patienten mit Plaque-Ruptur anhand von Alter (±5 Jahren), Geschlecht und Diabetes Mellitus Typ II zugeordnet. Aus den entnommenen lokalen und systemischen Blutproben wurden die neutrophilen Granulozyten für die funktionellen in-vitro Experimente isoliert. Mittels Durchflusszytometrie wurde eine Immunophänotypisierung der verschiedenen Neutrophilen-Rezeptoren durchgeführt. Die koronaren Thromben wurden auf die Expression von spezifischen Neutrophilen-Markern immunhistochemisch untersucht.

Obwohl es keine Unterschiede in der Absolutzahl der Neutrophilen zwischen Patienten mit Plaque-Erosion und Plaque-Ruptur gab, beobachteten wir eine erhöhte Toll-like Rezeptor 2 (TLR2) Expression auf den Neutrophilen der Plaque-Erosion Patienten. Nach Aktivierung des TLR 2 in-vitro sezernierten die neutrophilen Granulozyten der Patienten mit Plaque-Erosion mehr aktive Matrixmetalloproteinase 9 (MMP9). Ebenfalls zeigten sie eine gesteigerte Zytotoxizität gegenüber Endothelzellen als Hauptmerkmal der Plaque-Erosion. Hyaluronan kann als endogener Aktivator des TLR2 dienen (8). Passend dazu beobachteten wir eine erhöhte lokale Plasma-Konzentration von Hyaluronan (HA) in Patienten mit Plaque-Erosion, sowie eine erhöhte Expression des HA-generierenden Enzyms Hylauronidase 2 (HYAL2) in den Thromben der Patienten mit Plaque-Erosion.

Zusammenfassend beschreibt die aktuelle Studie neue spezifische Mechanismen der TLR2-vermittelten Aktivierung von neutrophilen Granulozyten im betroffenen Koronargefäß von Patienten mit Plaque-Erosion und stellt dadurch die Grundlage für die Entwicklung von gezielten therapeutischen und präventiven Ansätzen für diese Patientenpopulation.

Abstract

Background: Endothelial cell desquamation (ECD) due to inflammatory activation is one of the main pathophysiological features of acute coronary syndrome with intact fibrous cap (IFC-ACS, plaque erosion) (2, 5). The neutrophil granulocytes are the first immune cells to arrive at the coronary culprit lesion after ACS. Therefore, the current subanalysis of the OPTICO-ACS study aims to provide a better understanding of their molecular activation patterns.

Methods: Using optical coherence tomography (OCT) of the ACS-causing culprit lesion two groups (IFC-ACS vs. RFC-ACS) were generated, each consisting of thirty-two patients matched by age, gender and diabetes mellitus type II. Local and systemic blood samples were collected from the site of the ACS-causing culprit lesion (LOC) and from the arterial sheath (SYS). Quantification of neutrophil counts and expression of activation markers was carried out by flow cytometry. MMP9 activity was assessed by fluorescence-based zymography. The combined effect of MMP9 and disturbed flow conditions were studied in an Ibidi flow chamber imitating coronary bifurcations. The direct cytotoxic effects of TLR2 pre-activated neutrophils was examined in a co-culture with endothelial cells. Immunohistological staining of thrombus specimens characterized the expression of hyaluronidase 2 (HYAL2), an enzyme known to produce pro-inflammatory low molecular weight hyaluronan as one of the endogenous TLR2-ligands (9, 10).

Results: Neutrophils of IFC-ACS patients show significantly higher expression of the toll-like receptor 2 (TLR2) in comparison to RFC-ACS-derived neutrophils, despite an equal cell count. Furthermore, the MMP9 plasma activity is significantly higher in local samples from IFC-ACS patients, indicating secretion and proteolytic activation of the enzyme during ACS. Local IFC-ACS- derived neutrophils increased their secretion and activity rates of MMP9 in response to TLR2-stimulation using Pam3CSK4, which was reversible after TLR2 blockade by a monoclonal neutralizing antibody. However, the combination of MMP9 and turbulent flow conditions leads to significant ECD. Furthermore, the TLR2-activation increases the survival of local IFC-ACS derived neutrophils, which induce higher rates of endothelial cell death in co-culture, independently of TLR2. Last but not least, IFC-ACS derived thrombi show higher expression of HYAL2 with subsequent higher local plasma concentration of hyaluronic acid as one of the main endogenous TLR2-ligands.

Conclusion: By revealing novel local TLR2-dependant neutrophil activation patterns in IFC-ACS patients the current study provides new insights into the mechanism of plaque erosion. Moreover, the data suggest a crucial role of the hyaluronan metabolism in the endogenous activation of the TLR2 pathway in IFC-ACS. Further research is needed to assess the beneficial effects of a temporary TLR2-blockade in IFC-ACS and the possible application in secondary prevention.

1. Introduction

1.1. The Pathophysiology of Acute Coronary Syndrome with Intact Fibrous Cap (IFC-ACS, Plaque Erosion)

1.2. Prevalence of Plaque Erosion

Acute Coronary Syndrome (ACS) is defined as an insufficient oxygen supply to the myocardium due to a partial or total thrombotic coronary occlusion caused by either plaque rupture (45-65%), plaque erosion (30-50%) or, more rarely, calcified nodules (1-2%)(11).

In 1994 van der Wal et al. described eight out of twenty patients, who died from ACS and showed histological signs of plaque erosion (12). Some subsequent larger post-mortem studies confirmed the prevalence of plaque erosion in about 31% of fatal myocardial infarction patients (13). With modern intracoronary imaging modalities such as optical coherence tomography (OCT), it has become possible to characterize the culprit lesion in vivo, which opened the door to a better characterization and following application of personalized treatment approaches for this patients population. The OCT-based diagnosis of plaque erosion relies on exclusion of signs of plaque rupture or calcified nodules and it has been reported in around 41% of ACS patients (14).

1.3. Clinical Characteristics of Plaque Erosion

Generally, plaque erosion is more common in non ST-segment elevation myocardial infarction (NSTEMI) with 61.5% than in ST-segment elevation myocardial infarction (STEMI)(15). Using multivariate analysis Yamamoto et al. showed that the combination of the following five independent parameters increased the probability of plaque erosion to 73,1%: age<68 years, normal kidney function, absence of diabetes mellitus type 2, anterior ischemia and hemoglobin >15g/dl (1). A recent study by Seegers et al. disproved the hypothesis that plaque erosion is more common in younger women, but showed a similar distribution of the culprit plaque morphology in both sexes with a rising trend towards plaque rupture in older women (16).

1.4. Pathological Characteristics of Plaque erosion

From histological studies we know that plaque rupture arises from the so called ‘vulnerable plaques’ or ‘thin cap fibroatheromas’ (TCFAs), which are characterized by a large lipid core, less smooth muscle cells covering the core and a thin fibrous cap (<65µm)(17). Meanwhile, the coronary thrombosis in plaque erosion is triggered by a local detachment of endothelial cells on the surface of coronary plaques with intact fibrous caps and without the above-mentioned vulnerability features (7). Through excessive lipid lowering we directly address the pathological core of RFC-ACS and as a consequence we observe a rise in the prevalence of IFC-ACS in recent years (2).

Now the question arises which biological mechanisms may trigger superficial erosion?

Hemodynamic studies postulate coronary bifurcations with turbulent flow conditions as the predisposition locations for plaque erosion (18). Furthermore, it seems that multiple different hits are required as some animal studies suggest not only distinct flow conditions but their combination with neutrophils and activated endothelium as crucial for the initiation of plaque erosion (6, 7). Recently, some first in-human data suggested distinct local inflammatory patterns in the coronary vessel marked by elevated T-cell cytotoxicity with higher coronary distribution of CD4+ and CD8+ T cells as well as their pro-inflammatory metabolites as one of the characteristics of IFC-ACS (19).

1.5. Inflammation and plaque erosion

Inflammation and atherosclerosis have been associated since the very early years of coronary research, especially in the context of macrophages developing to foam cells by the uptake of oxidized low-density lipoprotein (oxLDL) as the pathological hallmark of the vulnerable plaque (7). In this context, modern atherosclerosis research advances this concept by showing us distinct inflammatory pathways typical for plaque rupture or erosion, allowing thereby to identify novel therapeutic targets.

The neutrophil granulocytes orchestrate the immune cascade after acute coronary syndrome through a regulated cytokine and granule content release(20). They are important immune modulators with both pro- and anti-inflammatory functions. Neutrophils are even capable of aggravating the coronary thrombosis by the release of neutrophil extracellular traps (NETs) during the process of controlled cell death known as NETosis (21).

Therefore, the current study focuses on the neutrophil activation patterns in patients with plaque erosion and plaque rupture, aiming to identify distinct pathological signatures suitable for targeted immune modulatory treatments in plaque erosion.

2. Methods

2.1. Study Design

The prospective, multicentre OPTICO-ACS registry examined patients with acute coronary syndrome (non-ST-elevation myocardial infarction, NSTEMI or ST-elevation myocardial infarction, STEMI) who are admitted to the hospital and undergoing percutaneous coronary intervention (PCI) in combination with OCT-imaging of the culprit lesion. The OPTICO-ACS registry studied not only the clinical outcomes and rates of major cardiac events in association with the culprit plaque morphology, but also the distribution of different immune cells and their cytokines, allowing for a deep characterization of the different ACS-phenotypes.

The study was registered at ClinicalTrials.gov under NCT03129503 and conducted after approval by the ethics committee of the Charitè University Berlin (No. EA1/270/16) after written informed consent of all participants. In total 557 patients where included according to the previously reported inclusion and exclusion criteria (5). Most importantly patients with other inflammatory/rheumatic or malignant co-morbidities were excluded in order to study inflammatory patterns in atherosclerosis only. After OCT-evaluation of the culprit lesion by two independent core labs 360 patients were considered suitable for study participation. The experiment operator was blinded to the underlying pathology.

For the purpose of the current sub-study 32 patients with plaque erosion were matched 1:1 to patients with plaque rupture by biological sex, age (± 5 years) and diabetes mellitus type 2 in order to minimize the previously observed biological heterogeneity in the main cohort as well as to control for known variables to affect the neutrophil response like aging, biological sex and diabetes mellitus type 2 (22-26) (Figure 1).

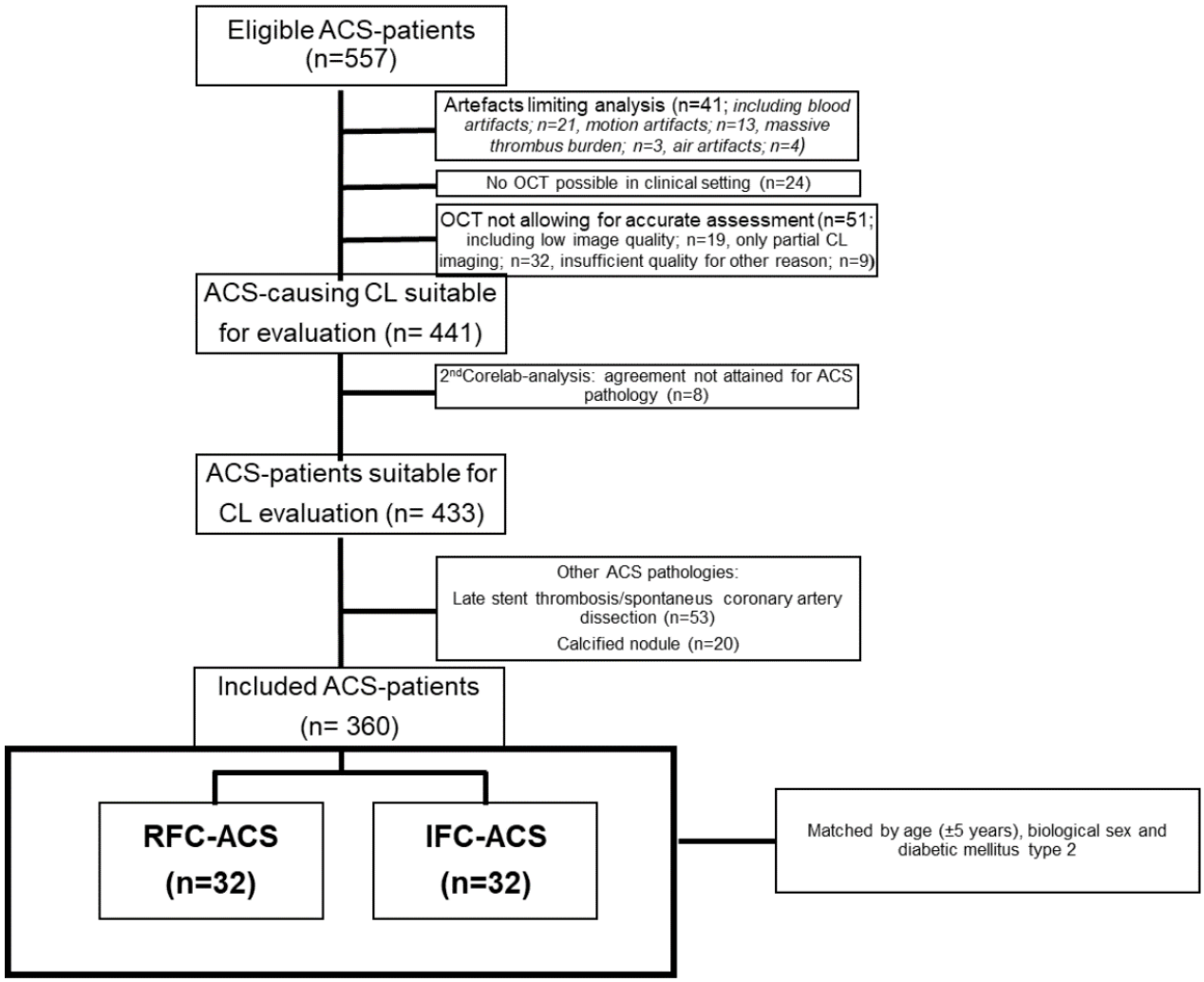

Figure 1: Study Flow Chart

Abbreviations: ACS: acute coronary syndrome, OCT: optical coherence tomography, CL: culprit lesion, RFC-ACS: acute coronary syndrome with ruptured fibrous cap, IFC-ACS: acute coronary syndrome with intact fibrous cap, n=number;

Own illustration modified from the original publication: Meteva et al., EHJ, 2023, *doi: 10.1093/eurheartj/ehad379*

2.2. Blood Sampling and Processing

Upon admission to the catheterization laboratory and before OCT-imaging and PCI, two blood samples were obtained from each patient: 30ml of local coronary blood collected by thrombectomy with the Export Advance aspiration catheter system (Medtronic, Minneapolis, MN, USA) and 50ml of systemic blood from the peripheral artery (Figure 2). Prior to the collection of the blood samples all patients received the standard intravenous med-

ical treatment for ACS with 70-140IE heparin /kg up to a maximal amount of 5000IE heparin in total and 150-300mg aspirin. Using a cell strainer with 70µm pores, thrombotic material was recovered from the local blood samples and washed twice in PBS, fixed in 4% paraformaldehyde for 15minutes, dehydrated in 30% sucrose for 10minutes and cryopreserved in OCT-mounting medium (Tissue Tek, Sakura, Japan) at -80°C for immunohistochemistry.

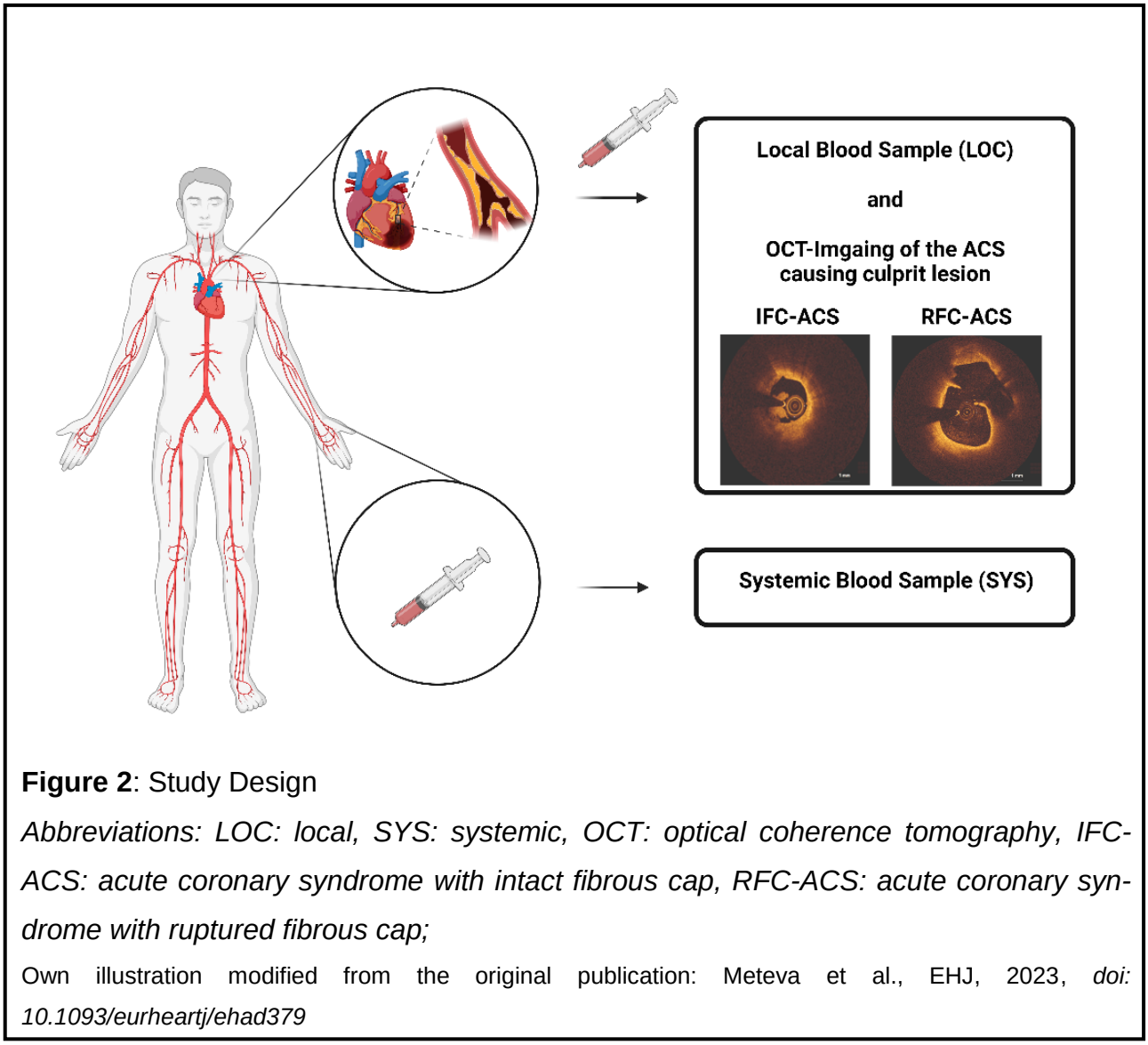

Figure 2: Study Design

Abbreviations: LOC: local, SYS: systemic, OCT: optical coherence tomography, IFC-ACS: acute coronary syndrome with intact fibrous cap, RFC-ACS: acute coronary syndrome with ruptured fibrous cap;

Own illustration modified from the original publication: Meteva et al., EHJ, 2023, *doi: 10.1093/eurheartj/ehad379*

Furthermore, 100µl of non-centrifuged EDTA blood was stained using our pre-defined flow cytometry antibody panel for a pre-selected set of neutrophil surface markers (Table 1) for 20minutes, fixed in 0.5% paraformaldehyde. The median fluorescence intensity (MFI) for each marker was measured 16-24h later on the Attune NxT Acoustic Focusing Flow Cytometer (Thermo Fischer, USA).

Table 1: Neutrophil Flow Cytometry Panel

Antibody	Supplier	Laser	Detector
CD284-BV421	Biolegend	violet (405 nm)	VL1 (440/50)
CD16-BV510	Biolegend	violet (405 nm)	VL2 (512/25)
CD11b-BV650	Biolegend	violet (405 nm)	VL3 (603/48)
CD45-BV711	BioLegend	violet (405 nm)	VL4 (710/50)
CD282-AF488	Biolegend	blue (488 nm)	BL1 (530/30)
VEGFR1-PE	Biolegend	blue (488 nm)	BL2 (574/26)
CXCR4-PE/Dazzle594	Biolegend	blue (488 nm)	BL3 (695/40)
CD88–PE/Cy7	Biolegend	blue (488 nm)	BL4 (780/60)

Abbreviations: CD: cluster of differentiation, VL: violet laser, BL: blue laser, VEGFR1: Vascular Endothelial Growth Factor Receptor 1, CXCR4: Chemokine Receptor Type 4;
Own illustration modified from the original publication: Meteva et al., EHJ, 2023, *doi: 10.1093/eurheartj/ehad379*

Data was analysed on the Kaluza v1.5 software (Beckmann Couter Inc, USA). The doublets were discriminated using forward scatter height (FSC-H) vs. width (FSC-W) gating. Afterwards the granulocytes were selected based on their high granularity using their typical side scatter height (SSC-H) profile. In the last step the MFI of each parameter was measured on the $CD16^{hi}$ neutrophil population (Figure 3).

The remaining blood was filled into EDTA- and citrate-anticoagulated tubes and centrifuged twice at 1200g for 10min at room temperature (20-25°C) to generate platelet free plasma, which was preserved in sterile cryotubes at -80°C for long-term preservation and further measurements.

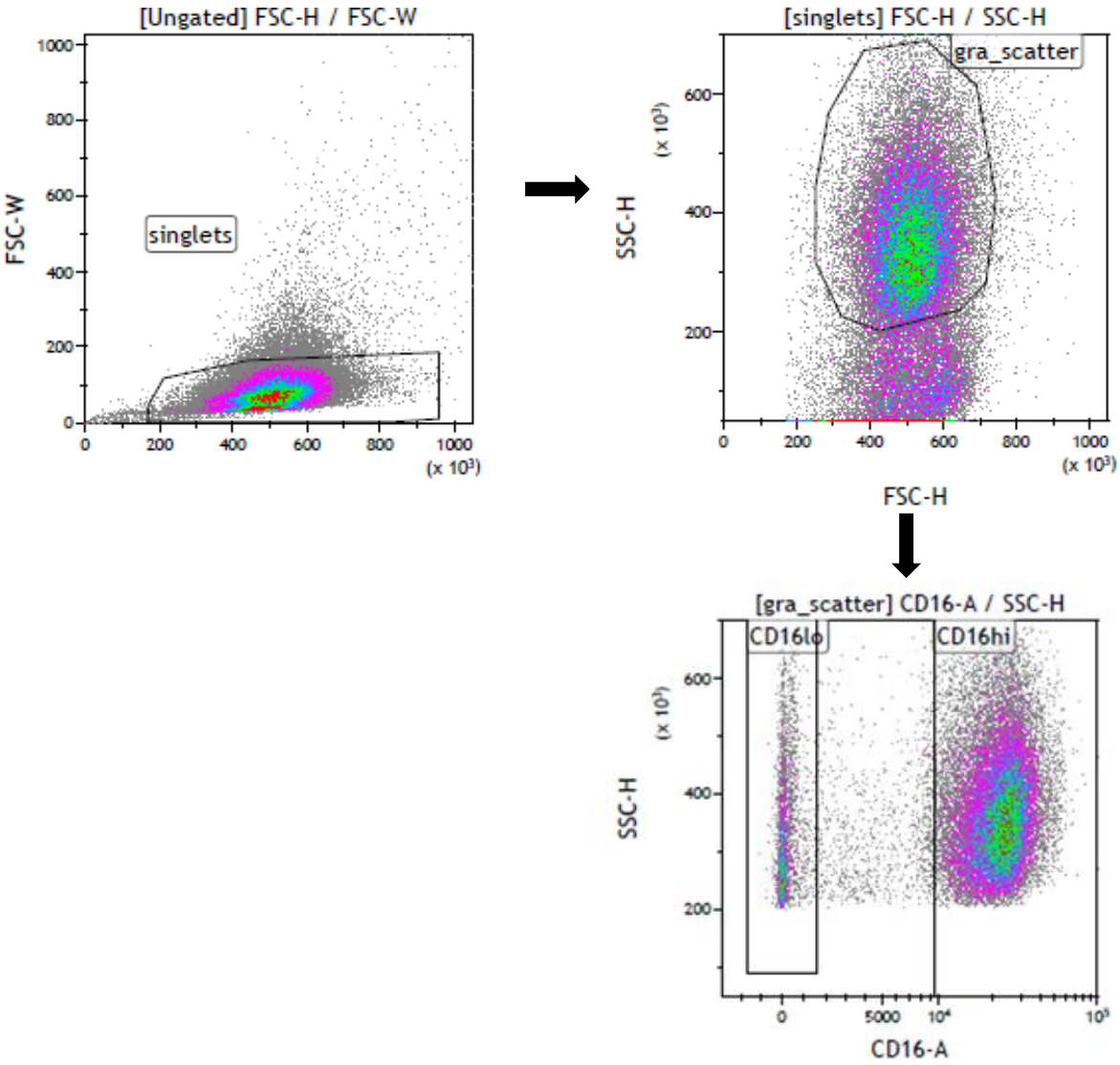

Figure 3: Flow Cytometry Gating Strategy

Abbreviations: FSC-H/W: forward scatter-height/width; SSC-H: side scatter-height; lo: low; hi: high;

Own illustration modified from the original publication: Meteva et al., EHJ, 2023, doi: 10.1093/eurheartj/ehad379

2.3. Neutrophil Isolation

Fresh local and systemic heparin-anticoagulated blood samples from the above mentioned patients were used for isolation of polymorphnuclear neutrophils (PMNs) with the density centrifugation technique using the Polymorphprep medium (Alere Technologies, Oslo, Norwegen). First, the whole blood was carefully layered on the top of the medium in a ratio 1:1 in 15ml sterile tubes and centrifuged at 500g, Acceleration 1, Deceleration

1 for 35min allowing for visual separation of the PMNs, which were further collected in a separate tube with fresh cold PBS. Secondly, remaining erythrocytes were lysed with cold distilled water in a volume ratio 1:1 for 30 sec (for example 10ml of neutrophil suspension and 10ml of distilled water). Physiological osmolality was immediately restored by adding the same amount of 2x cold PBS. Cells were washed at 300g, Acceleration 9, Deceleration 9 for 5min. The viability and cell count of isolated PMNs were assessed by staining with propidium iodide (PI) and flow cytometry assessment. The cells were kept on ice for further experiments in Roswell Park Memorial Institute (RPMI) 1640 Medium, supplemented with 4-(2-hydroxyethyl)-1-piperazineethane sulfonic acid (HEPES), pyruvate, 4.5g glucose, 0.5% fetal bovine serum (FBS) and 1% penicillin/streptomycin (Thermo Fisher Scientific, USA).

2.4. Plasma Concentration of Metabolites of Interest

The concentration of matrix metalloproteinase 9 (MMP9) was assessed in citrate-anticoagulated plasma samples using an enzyme-linked immunosorbent assay (catalogue number: BMS2016-2TEN, MMP 9 Human ELISA, Thermo Fischer, USA) according to the manufacturer's instruction. Furthermore, we measured the concentration of neutrophil-gelatinase associated lipocalin (NGAL), which is a known stabilizer of MMP9, in EDTA-plasma samples using the Human NGAL ELISA Kit (catalogue number: KIT 036CE from Bioporto, Hamburg). Using a non-competitive ELISA-like technique (catalogue number: 029-001, Corgenix, Broomfield, CO, USA), the hyaluronic acid (HA) plasma levels were measured in EDTA-plasma samples.

2.5. MMP9 Activity Measurement

The enzymatic activity of MMP9 after activation of the isolated neutrophils was measured in supernatants by fluorescence gelatine zymography using the EnzCheck Gelatinase/Collagenase Assay Kit according to the manufacturer's instructions (catalogue number: E12055, Invitrogen, Fisher Scientific, Göteborg, Sweden). $1x10^4$ of isolated neutrophils in OPTI-MEM medium supplemented with 5mM $CaCl_2$ (Reduced serum medium, catalogue number: 11058021, Thermo Fischer, USA) were activated by a human recombinant TLR2/1 agonist Pam3CSK4 at a final concentration: 500ng/ml (Invivogen, USA) for a total time of 120 minutes. The control group was pre-treated with a selective inhibitory anti-TLR2 antibody (mouse monoclonal IgG1 anti-human antibody to TLR2, clone

T2.5) at a final concentration of 1.25µg/ml (catalogue number ab16894, Abcam, Cambridge, England) for 15min prior to activation with Pam3CSK4 as described above. In the beginning of the assay the fluorescence marked DQ gelatine was added to the samples in a ratio 1:1. The samples were incubated at 37.3°C in the spectrophotometer plate reader (Tecan, Switzerland) and measured after pre-selected time points with an absorption maxima at 485nm and the fluorescence emission was measured at 530nm. The activity of the commercially available Clostridium histolyticum collagenase, provided with the assay kit, was used as a positive control enzyme according to the manufacturer's instruction.

2.6. Co-Culture of Neutrophils and Human Aortic Endothelial Cells

In order to assess the TLR2-dependant cytotoxic effect of neutrophils on human aortic endothelial cells (HAECs) a co-culture assay of $1x10^6$ as previously described pre-treated neutrophils on a monolayer of $1x10^5$ commercially available human aortic endothelial cells passage 7 (Lonza, Basel, Switzerland) was established for 24h. The endothelial cells were initially grown to 80-90% confluence in 12-well-cell-culture plates using endothelial cell growth medium (EGM, Lonza, Basel, Switzerland), supplemented with 10% fetal calf serum (FCS) and 1% penicillin/streptomycin. Prior to the co-culture experiment the endothelial cells were pre-conditioned in growth-factor deprived and low serum (0,5% FCS) in order to increase their reactivity towards the neutrophils. After 24h of co-incubation the cells were harvested into suspension using trypsin/EDTA and afterwards immediately stained for 15minutes with Sytox Orange (Thermo Fischer, USA) as a nucleic acid stain, Annexin V-Pacific Blue for detection of apoptosis, anti-human CD45-BV711 for detection of leucocytes, CD146-AF488 for detection of endothelial cells, anti-CD16 PerCP/Cy5.5 for detection of neutrophils (all antibodies from BioLegend, San Diego, USA). The rates of live/apoptotic/dead endothelial cells was estimated on the Attune NxT Acoustic Focusing Flow Cytometer (Thermo Fischer, USA) immediately after staining by co-expression of AnnexinV and Sytox Orange as shown in Figure 4.

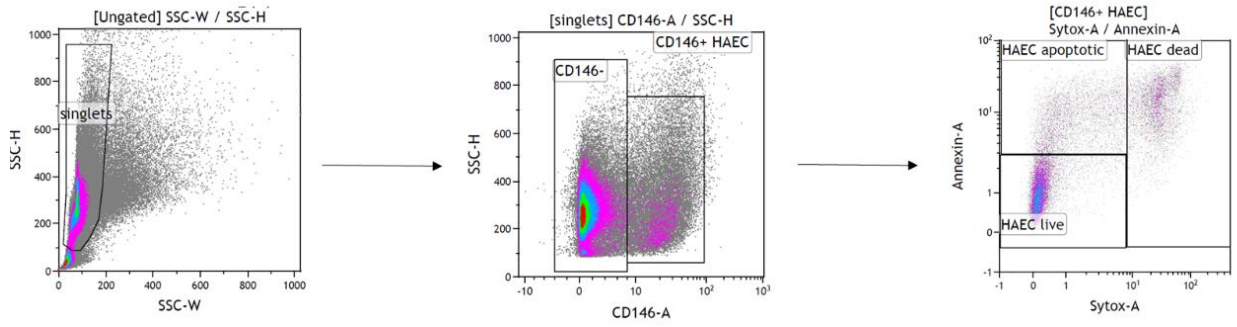

Figure 4: Apoptosis Assay Gating Strategy

Abbreviations: FSC-H/W: forward scatter-height/width, SSC-H/W: side scatter-height/width, HAEC: human aortic endothelial cells, CD: cluster of differentiation;

Own illustration modified from the original publication: Meteva et al., EHJ, 2023, doi: 10.1093/eurheartj/ehad379

2.7. Assessment of Neutrophil Survival upon TLR2 Activation

Furthermore, we assessed the survival of neutrophils after 24hours of TLR2 activation indirectly by measuring the shedding of CD16 as a marker of apoptosis (27). For this purpose we divided the neutrophil population into $CD16^{hi}$ and $CD16^{lo}$ neutrophils, based on their CD16 expression and gated the proportion of live, apoptotic and dead neutrophils for both subpopulations according to the same gating strategy as described in Figure 4. Figure 5 shows a graphical summary and a representative analysis of the live/apoptotic/dead percentages in both $CD16^{hi}$ and $CD16^{lo}$ neutrophil populations.

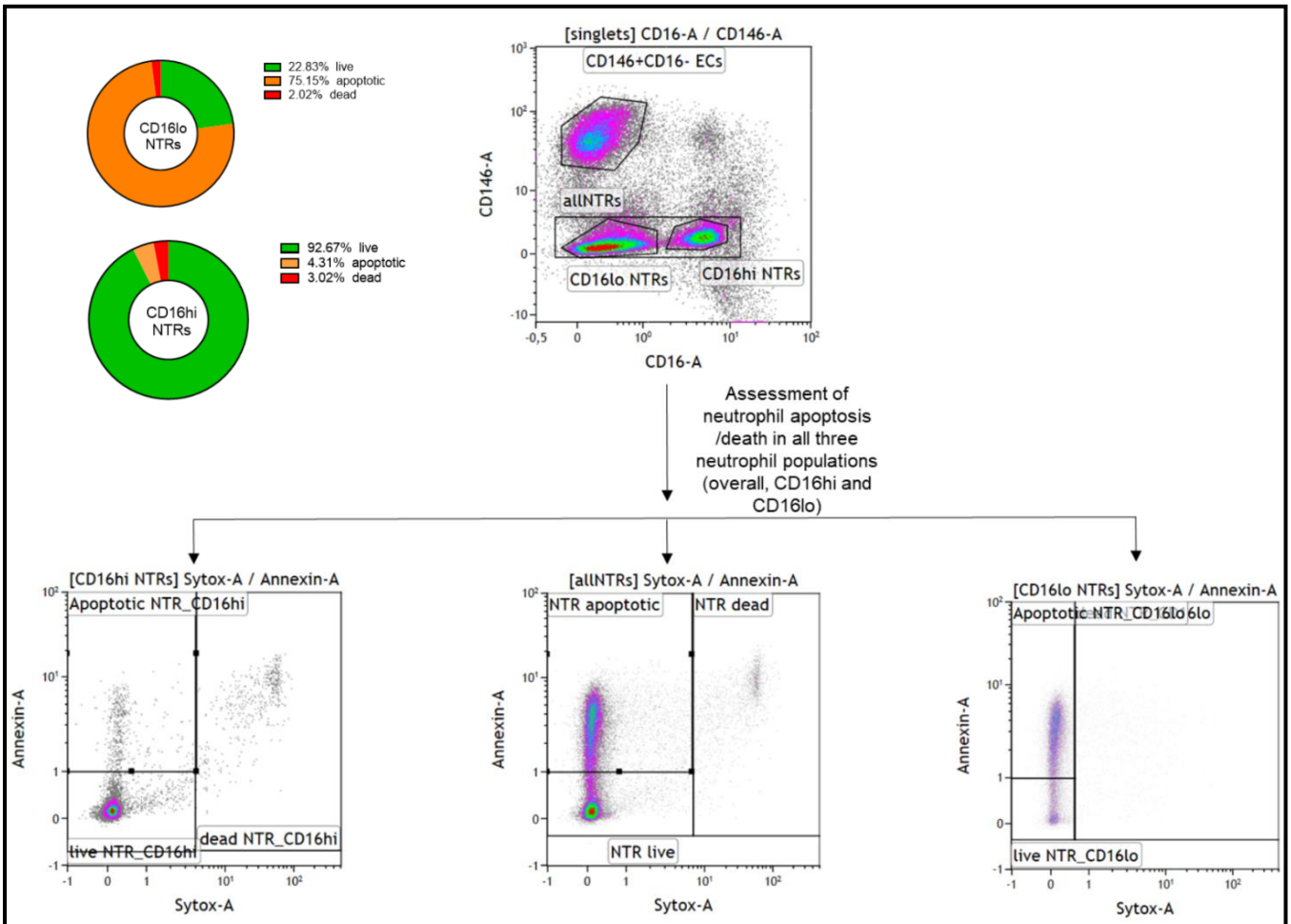

Figure 5: Assessment of Neutrophil Survival Gating Strategy

Abbreviations: NTRs: neutrophils, lo: low, hi: high, CD: cluster of differentiation;

Own illustration modified from the original publication: Meteva et al., EHJ, 2023, doi: 10.1093/eurheartj/ehad379

2.8. Analysis of Flow conditions on Endothelial Cell Detachment in Combination with MMP9

Using the Ibidi Flow Chamber System (Gräfelfing, Germany) with endothelial cell monolayers grown in double-y-shaped microchannel slides coated with 1% gelatine we tested two different flow conditions: laminar defined as unidirectional flow with 12dyn/cm^2 or oscillatory defined as bidirectional flow with 12dyn/cm^2 and the simultaneous effect of human recombinant MMP9 at a final concentration of 500ng/ml (Enzo Lifesciences, New York, USA) on endothelial cell detachment after 24hours. For this purpose, the slides were stained with phalloidin for F-actin and Hoechst for cell nuclei. Images were taken on

a BZ-9000 inverted fluorescence phase contrast microscope (Keyence, USA) in 10x magnification and endothelial cell detachment was assessed by ImageJ software version 1.48 (University of Wisconsin, USA).

2.9. Immunohistochemistry of Thrombus Specimens

OCT-embedded thrombus aspirates from twenty patients with plaque erosion and twenty patients with plaque rupture were cut into 5µm sections and were stained with a primary anti-HYAL2 antibody (1:500, Abcam, Cambridge, UK) at 4 °C overnight after treatment with antigen retrieval solution (CAT. N°. 00-4955-58, Thermo Fisher Scientific, Inc. Waltham, MA, USA) in a pre-heated water bath and after permeabilization with 1% Triton X-100 (Sigma-Aldrich, St. Louis, MO, USA). In order to block non-specific bindings we applied 0,5% Bovine Serum Albumin (BSA, Thermo Fisher Scientific, Inc. Waltham, MA, USA) for 15 minutes. The staining with the goat anti-rabbit secondary antibody conjugated to Alexa Fluor 546 (1:500; Thermo Fisher Scientific, Waltham, MA, USA) was carried out on the next day for a total incubation time of 90 minutes. For nuclei detection staining with 4′,6-diaminophenyl-indole (DAPI) (Invitrogen, Carlsbad, CA, USA) was used for 10 minutes. At the end the sections were preserved with ibidi mounting medium (ibidi GmbH, Gräfelfing, DE, EU) and images acquired on an Eclipse T-i2 microscope using 20x and 3x magnification (Nikon Corp., Tokyo, JP). Fiji Image J and NIS-Elements (Mager Scientific, Dexter, MI, USA) software was used for image processing. A representative image is shown in Figure 6.

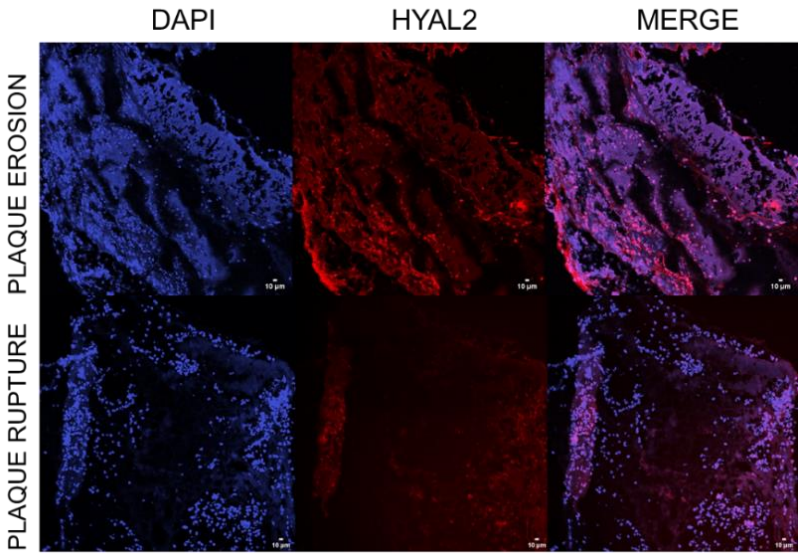

Figure 6: Immunohistochemistry Analysis of IFC-ACS vs. RFC-ACS- derived Thrombi

Abbreviations: DAPI: 4',6-diaminophenyl-indole; HYAL2: hyaluronidase 2;

Own illustration modified from the original publication: Meteva et al., EHJ, 2023, doi: 10.1093/eurheartj/ehad379

3. Statistical Analysis

In order to minimalize the biological heterogeneity of the neutrophil function resulting from different age, gender and diabetes mellitus type 2 status we chose a matched case-control study design.

Comparisons between two groups of continuously distributed variables were carried out using the Wilcoxon matched-pairs signed rank test, while categorical variables were analysed by Mc Nemar chi² test (28). Multiple comparisons within a patient including a factor (for example treatment or plaque phenotype) were carried out by a repeated measures analysis of variance (Repeated measures ANOVA). The multiple post-hoc comparisons aimed to detect a group difference at each time point and were corrected for multiple comparisons using the Bonferroni's post-hoc test. Results were considered significant at a two-sided p-value <0.05. The overall effect of the variables and their interaction was reported in the figure legends by using Cohen's d (standardized mean difference (SMD)) for pairwise comparisons with the following rule of thumb: $d < 0.2$ small effect, d between 0.2 and 0.8 medium effect, $d > 0.8$ large effect. For the analysis of variance (ANOVA) we reported the partial η^2 to measure the effect size, as it describes to which extent the total variance of outcome is explained by the covariates.

SAS 9.3 and GraphPad Prism Software (La Jolla, CA) were used for statistical analysis.

4. Results

4.1. Clinical Patients Characteristics and OCT Parameters

In general we did not observe any relevant differences in the patient's clinical characteristics between the two disease pathologies, besides the higher proportion of dyslipidaemia (94% vs. 68% in RFC-ACS vs. IFC-ACS, p=0.002) and correspondingly higher total (204±61 vs. 179±50.2 in RFC-ACS vs. IFC-ACS, p=0.04) and LDL (129±53 vs. 113±44.5 in RFC-ACS vs. IFC-ACS, p=0.026) cholesterol levels in patients with RFC-ACS vs. IFC-ACS (see table 2). Correspondingly, the pre-clinical use of statins was higher in the RFC-ACS cohort (9.4% vs. 3.1% in RFC-ACS vs. IFC-ACS; p= 0.01, see table 2).

Table 2: Clinical Characteristics

	RFC-ACS	**IFC-ACS**	**p**
Patient characteristics:			
Age (years)	62.0 ± 16.75	61.0 ± 16.5	0.793
Male (n;%)	26 (81%)	26 (81%)	0.999
Family history for CAD (n;%)	14 (44%)	14 (44%)	0.999
Active Smoking (n;%)	13 (40%)	17 (53%)	0.459
Diabetes mellitus Type 2 (n;%)	7 (22%)	7 (22%)	0.999
Arterial hypertension (n;%)	29 (91%)	26 (81%)	0.214
Dyslipidemia* (n;%)	30 (94%)	22 (68%)	**0.002**
BMI (kg/m2)	25.5 ± 6.1	25.6 ± 3.9	0.652
Previous History of PCI (n;%)	6 (19%)	1 (3%)	0.071
Laboratory data:			
Total cholesterol (TC) (mg/l)	204.0 ± 61.0	179.0 ± 50.2	**0.040**
LDL cholesterol (LDL-C) (mg/l)	129.0 ± 53.0	113.0 ± 44.5	**0.026**
HDL cholesterol (HDL-C) (mg/l)	40.0 ± 14.0	50.0 ± 20.0	0.417
Serum creatinine (mg/l)	0.94 ± 0.2	0.97 ± 0.2	0.256
Hemoglobin (g/dl)	14.7 ± 1.8	14.8 ± 1.6	0.681
Leukocytes (per nl)	10.5 ± 4.3	11.0 ± 6.0	0.367
hsCRP (mg/l)	2.1 ± 5.4	2.0 ± 3.2	0.721
ACS characteristics:			
Presentation as STE-ACS (n;%)	20 (63%)	18 (50%)	0.298
CK peak (U/l)	902.0 ± 720	569.0 ± 1.063	0.267

LV-EF at discharge (%)	59.0 ± 11	55.0 ± 12.5	0.382
Concomitant Medication:			
PCSK9-inhibitor (n; %)	0 (0%)	0 (0%)	0.241
Ezetimibe (n; %)	0 (0%)	1 (3.1%)	0.191
Statín (n; %)	3 (9.4%)	1 (3.1%)	**0.010**

*Abbreviations: RFC-ACS: Ruptured fibrous cap – acute coronary syndrome, IFC-ACS: Intact fibrous cap acute coronary syndrome, SD: standard deviation, n: number, BMI: body mass index, LVEF: left ventricular ejection fraction, hsCRP: high sensitive C-reactive protein, CK: creatinine kinase, LDL: low density lipoprotein, HDL: high density lipoprotein, STE-ACS: ST-elevation myocardial infarction, PCI: percutaneous coronary intervention; * defined as total cholesterol ≥220mg/dl, triglycerides≥150mg/dl, LDL-C ≥140mg/dl, HDL-C ≤40mg/dl or taking medication for dyslipidemia;*
Own illustration modified from the original publication: Meteva et al., EHJ, 2023, doi: 10.1093/eurheartj/ehad379

The matched study cohort was considered representative of the whole cohort in terms of comparability (see table 3). The data sets were not tested for statistical significance as the matched cohort being part of the entire cohort, which does not allow for proper statistical analysis.

Table 3: Clinical Characteristics of the Matched and Entire Study Cohort.

	Entire Cohort (n=360)	**Matched Cohort** (n=64)
Age (years)	62.5 ± 12.0	62.1 ± 11.7
Male (n;%)	267 (74%)	52 (81%)
Family history for CAD (n;%)	138 (38%)	28 (44%)
Active Smoking (n;%)	158 (44%)	30 (47%)
Diabetes mellitus type 2 (n;%)	68 (19%)	14 (22%)
Arterial hypertension (n;%)	276 (77%)	55 (86%)
Dyslipidemia (n;%)	255 (71%)	52 (82%)
BMI (mean±SD)	27.3 ± 4.4	26.8 ± 5.0
Previous History of PCI (n;%)	35 (1%)	7 (1%)
Total cholesterol (mg/l; mean±SD)	182.2 ± 41.4	190.6 ± 42.6
LDL cholesterol (mg/l; mean±SD)	121.6 ± 38.1	128.1 ± 35.0
HDL cholesterol (mg/l; mean±SD)	46.4 ± 14.9	46.3 ± 15.3
Serum creatinine(mg/l; mean±SD)	1.0 ± 0.2	0.9 ± 0.2
Leukocytes (per nl)	11.5 ± 3.9	11.4 ± 4.0
hsCRP (mg/l; mean±SD)	12.5 ± 34.7	4.0 ± 5.4

Presentation as STE-ACS (n;%)	225 (63%)	38 (59%)
CK peak (U/l; mean±SD)	1417.2 ± 1575.9	1237.8 ± 1562.7
LV-EF at discharge(%; mean±SD)	55 ±10	56 ± 9
Abbreviations: CAD: coronary artery disease, BMI: body mass index, PCI: percutaneous coronary intervention; LDL: low-density lipoprotein; HDL: high-density lipoprotein; hsCRP: high sensitive C-reactive protein; STE-ACS: ST-elevation myocardial infarction; CK: creatinine kinase; LV-EF: left ventricular ejection fraction; Own illustration modified from the original publication: Meteva et al., EHJ, 2023, doi: 10.1093/eurheartj/ehad379		

Furthermore, the standardized mean difference (SMDs, d) between the continuous baseline characteristics of the two disease groups demonstrated well-balanced disease populations with small effect sizes apart from the total and the LDL cholesterol, which are showing a medium effect size d (see table 4).

Table 4: SMDs of the Baseline Characteristics of the Study Populations

	RFC-ACS	**IFC-ACS**	**d**
PCI characteristics:			
Total Stented Length (mm)	26.0 ± 30.6	23.0 ± 11.5	**0.08**
Largest Stent Diameter (mm)	3.5 ± 0.50	3.4 ± 1.0	**0.05**
Patient characteristics:			
Age (years)	62.0 ± 16.75	61.0 ± 16.5	**0.04**
BMI (kg/m2)	25.5 ± 6.1	25.6 ± 3.9	**0.08**
Laboratory data:			
Total cholesterol (mg/l)	204.0 ± 61.0	179.0 ± 50.2	**0.49**
LDL cholesterol (mg/l)	129.0 ± 53.0	113.0 ± 44.5	**0.56**
HDL cholesterol (mg/l)	40.0 ± 14.0	50.0 ± 20.0	**0.23**
Serum creatinine (mg/l)	0.94 ± 0.2	0.97 ± 0.2	**0.17**
Hemoglobin (g/dl)	14.7 ± 1.8	14.8 ± 1.6	**0.09**
Leukocytes (per nl)	10.5 ± 4.3	11.0 ± 6.0	**0.16**
hsCRP (mg/l)	2.1 ± 5.4	2.0 ± 3.2	**0.19**
ACS characteristics:			
CK peak (U/l)	902.0 ± 720	569.0 ± 1.063	**0.13**
Abbreviations: RFC-ACS: acute coronary syndrome with ruptured fibrous cap; IFC-ACS: acute coronary syndrome with intact fibrous cap; PCI: percutaneous coronary intervention; BMI: body mass index, LDL:			

low density lipoprotein; HDL: high density lipoprotein; hsCRP: high sensitive C-reactive protein; ACS: acute coronary syndrome; CK: creatinine kinase, SMDs: standardized mean difference, d; Own illustration modified from the original publication: Meteva et al., EHJ, 2023, doi: 10.1093/eurheartj/ehad379

The OCT-analysis did not show any significant differences in the plaque composition and morphology between IFC-ACS and RFC-ACS, apart from the well-known features of the thin cap fibroatheroma which are typical for RFC-ACS lesions. In this regard, 97% of the RFC-ACS patients had a TCFA, while only 16% of the IFC-ACS patients exhibited the features of a thin-cap fibroatheroma. Correspondingly, the mean thickness of the fibrous cap was higher in IFC-ACS vs. RFC-ACS, while the maximum lipid arc greater in RFC-ACS vs. IFC-ACS (see table 5).

Table 5: OCT-Characteristics of RFC-ACS vs. IFC-ACS

	RFC-ACS	**IFC-ACS**	**p**
OCT-culprit lesion characteristics:			
MLA (mm²)	1.8 ± 0.6	1.9 ± 1.1	0.380
Thrombus characteristics:			
CL-associated thrombus formation (n;%)	32 (100%)	32 (100%)	-
Thrombus score	111.5 ± 55.5	71.5 ± 99.2	0.063
Culprit Plaque characteristics :			
Fibroatheroma (n;%)	32 (100%)	30 (94%)	0.157
Thin-cap fibroatheromas (n;%)	31 (97%)	5 (16%)	**0.001**
Mean FC thickness (μm)	53.5 ± 10.2	122.2 ± 89.2	**0.001**
Max lipid arc (°)	298.2 ± 62.1	221.0 ± 123.9	**0.001**
Calcification:			
Max calcium arc (°)	73.2 ± 121.05	94.5 ± 98.3	0.594
Mean calcified length (mm)	3.2 ± 8.0	4.5 ± 6.4	0.777

** The cut-off used to define proximity to bifurcations was 3mm.*
Abbreviations: CL: culprit lesion, RFC-ACS: ruptured fibrous cap acute coronary syndrome, IFC-ACS: intact fibrous cap-acute coronary syndrome, SD: standard deviation, n: number, MLA: minimum lumen area, FC: fibrous cap; Own illustration modified from the original publication: Meteva et al., EHJ, 2023, doi: 10.1093/eurheartj/ehad379

4.2. Immunophenotyping of Neutrophils by Flow Cytometry

In order to characterize the receptor expression of the neutrophil population we performed a flow cytometry analysis of different receptors usually expressed by neutrophils (please refer to section 'Methods' for further information on the panel) and observed a higher expression of the toll-like receptor 2 (TLR 2) on local and systemic IFC-ACS derived neutrophils in comparison to RFC-ACS derived neutrophils (LOC IFC-ACS vs. LOC RFC-ACS: 2004±485 vs. 1502±599, p=0.011; SYS IFC-ACS vs. SYS RFC-ACS: 2042±533 vs. 1540±622, p=0.007). The cell count was not different between the two pathologies as well as the expression of the other markers (see table 6). We observed a medium overall effect size of the TLR2 expression (see figure 7).

Table 6: Neutrophil Receptor Expression

	LOC IFC-ACS	**LOC RFC-ACS**	**P**	**SYS IFC-ACS**	**SYS RFC-ACS**	**P**
SSC-H^{hi}CD16^{hi} Neutrophils	38233± 37240	39180±26871	0.993	42778±38809	41989±33382	0.875
SSC-H MFI	370409± 93772	392766±109894	0.536	401498±78289	418143±92328	0.875
CD282 MFI	2004±485	1502±599	**0.011**	2042±533	1540±622	**0.007**
CD11b MFI	105.7±133.4	105.8±358.3	0.343	105.8±186.6	114.8±326.6	0.410
CXCR4 MFI	4509±1100	4349±1191	0.638	4531±1829	4378±1224	0.379
CD 16 MFI	20491±8054	22513±7865	0.432	22403±8140	2282±9129	0.561
CD284 MFI	105.5±0.1	105.5±0.2	0.367	105.5±0.1	105.5±0.3	0.453
VEGFR1 MFI	1420±410	1363±446	0.379	1503±547	1383±406	0.270
CD88 MFI	16989±7784	17529±8274	0.246	17255±9889	18278±5967	0.421
CD36 MFI	313.2±126.4	328.5±173.9	0.133	332.5±126.1	327.3±151.1	> 0.999

ABCG1 MFI	648.7±405	634.6±723.9	0.172	791.8±617.7	724.7±800.7	0.091
ABCA1 MFI	105.3±0.1	105.3±0.2	0.552	105.3±0.2	105,3±0.5	0.552
CD49d MFI	3321±1079	3302±839	0.331	3520±1158	3389±1002	0.224
CD49a MFI	105.7±0.2	105.7±0.1	0.362	105.7±4.8	105.8±5.7	0.729
CD11a MFI	74634±25099	71786±25228	0.692	77100±23.013	76254±22213	0.651

Abbreviations: SSC-H: side scatter height, CD: cluster of differentiation, MFI: median fluorescence intensity, CD 282: Toll-like receptor 2, CD284: Toll-like receptor 4,
Own illustration modified from the original publication: Meteva et al., EHJ, 2023, doi: 10.1093/eurheartj/ehad379

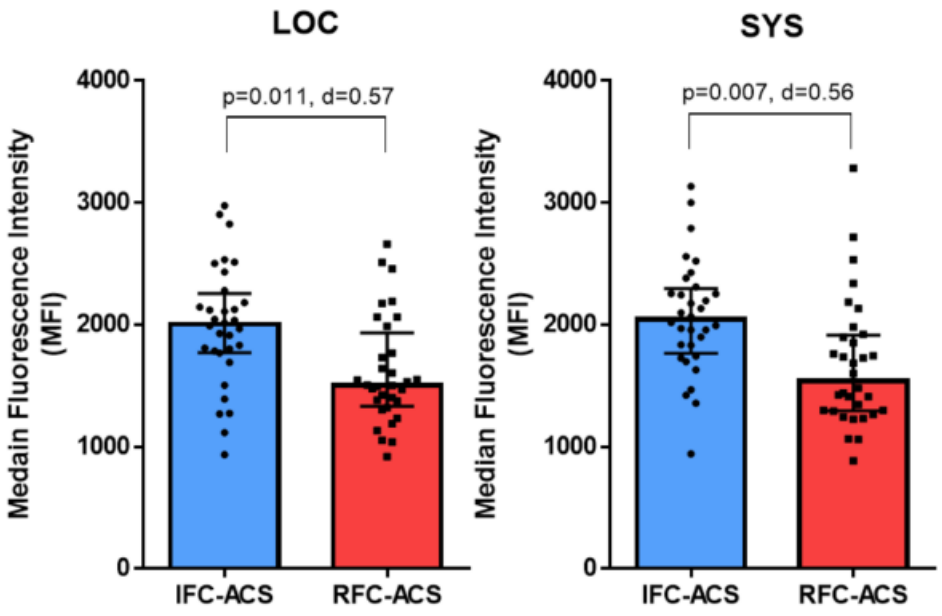

Figure 7: TLR2 Expression on Neutrophils in IFC-ACS vs. RFC-ACS

d < 0.2 small effect, d between 0.2 and 0.8 medium effect, d > 0.8 large effect; Values are expressed as median with interquartile range (IQR); Wilcoxon matched-pairs signed rank test; Abbreviations: LOC: local, SYS: systemic; RFC-ACS: acute coronary syndrome with ruptured fibrous cap; IFC-ACS: acute coronary syndrome with intact fibrous cap;

Own illustration modified from the original publication: Meteva et al., EHJ, 2023, doi: 10.1093/eurheartj/ehad379

4.3. MMP9 Secretion upon TLR2 Stimulation

In order to estimate the functional effect of TLR2 activation on the secretion of matrix metalloproteinase 9 (MMP9) we stimulated the isolated neutrophils from patients with IFC-ACS and RFC-ACS with a TLR2 agonist Pam3CSK4 and assessed the secretion of MMP9 as a response in a time course over 120min using a fluorescence-based gelatine zymography.

We observed a higher gelatinolytic activity, corresponding to higher MMP9 production and activation upon TLR2 stimulation in local neutrophils from IFC-ACS patients than in systemic or in RFC-ACS patients in general (see figure 8). The effect size measurement after repeated measures ANOVA shows a large effect of the pathology and the localization on the MMP9 production in stimulated neutrophils.

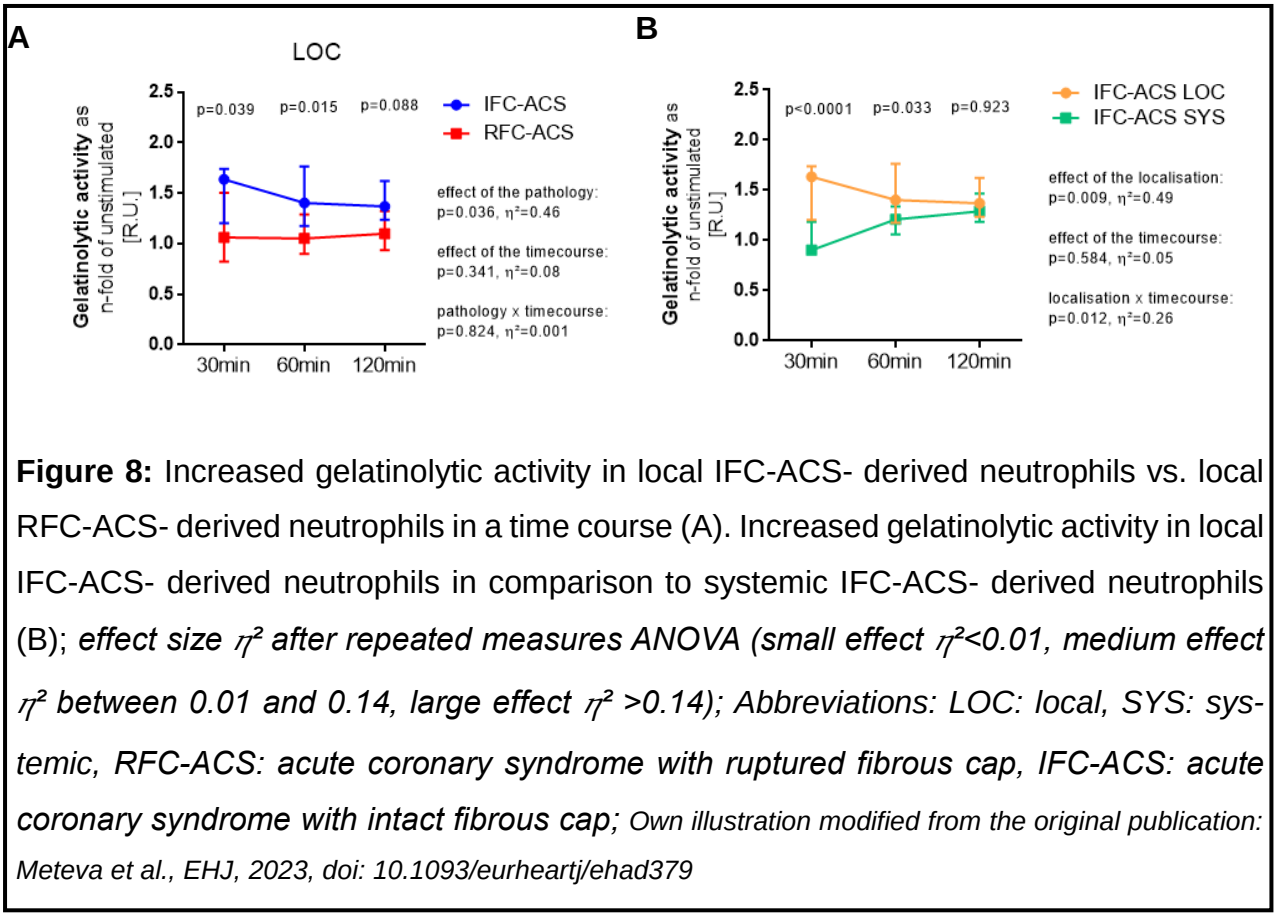

Figure 8: Increased gelatinolytic activity in local IFC-ACS- derived neutrophils vs. local RFC-ACS- derived neutrophils in a time course (A). Increased gelatinolytic activity in local IFC-ACS- derived neutrophils in comparison to systemic IFC-ACS- derived neutrophils (B); *effect size η^2 after repeated measures ANOVA (small effect η^2<0.01, medium effect η^2 between 0.01 and 0.14, large effect η^2 >0.14); Abbreviations: LOC: local, SYS: systemic, RFC-ACS: acute coronary syndrome with ruptured fibrous cap, IFC-ACS: acute coronary syndrome with intact fibrous cap;* *Own illustration modified from the original publication: Meteva et al., EHJ, 2023, doi: 10.1093/eurheartj/ehad379*

The observed effect was completely reversible in IFC-ACS patients (figure 9A) through an upstream selective blockade of TLR2 with a specific anti-TLR2 antibody vs. unspecific IgG control showing a TLR2-dependant increase in MMP9 production especially in IFC-ACS and not in RFC-ACS (see figure 9A and B).

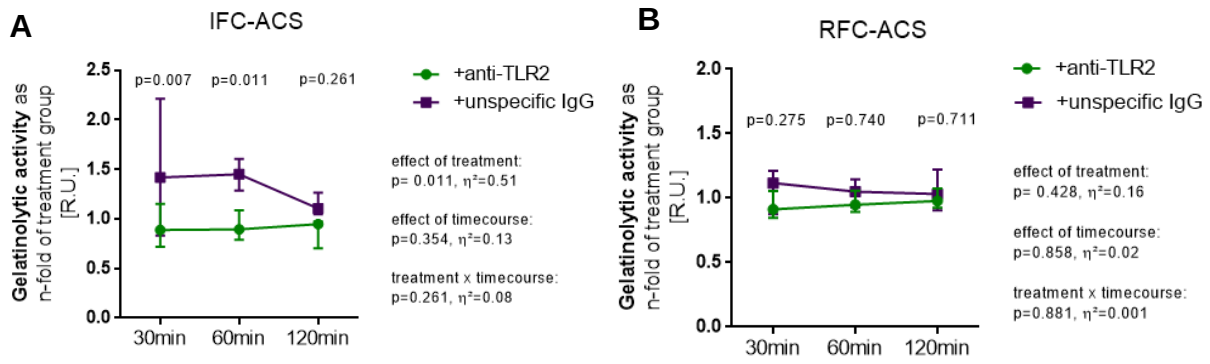

Figure 9: Anti-TLR2 pre-treatment reverses gelatinolytic activity in IFC-ACS- derived neutrophils; A) An anti-TLR2 pre-treatment reverses the effect of a TLR2 stimulation on local IFC-ACS- derived neutrophils in terms of gelatinolytic activity to the baseline level (B) No effect of anti-TLR2 pre-treatment of RFC-ACS neutrophils; *small effect η^2<0.01, medium effect η^2 between 0.01 and 0.14, large effect η^2 >0.14; Abbreviations: RFC-ACS: ruptured fibrous cap acute coronary syndrome; IFC-ACS: intact fibrous cap-acute coronary syndrome; Own illustration modified from the original publication: Meteva et al., EHJ, 2023, doi: 10.1093/eurheartj/ehad379*

Furthermore, we determined the expression of MMP9 vs. MMP2 in the supernatants of the stimulated neutrophils using size discrimination by gelatine zymography, conforming MMP9 to be the pre-dominant matrix metalloproteinase produced by TLR2-activated neutrophils (see figure 10).

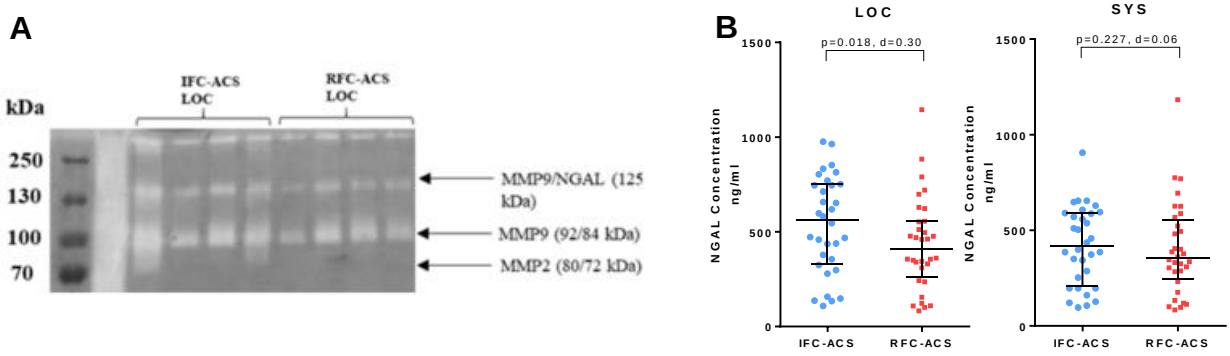

Figure 10: A) Representative image of gelatine zymography demonstrating the pre-dominance of MMP9 (92/84kDa) over MMP2 (80/72 kDa) in the neutrophil supernatants upon TLR2-stimulation B) Local and systemic concentrations of NGAL*; d < 0.2 small effect, d between 0.2 and 0.8 medium effect, d > 0.8 large effect; Abbreviations: LOC: local; SYS: systemic; RFC-ACS: ruptured fibrous cap acute coronary syndrome; IFC-ACS: intact fibrous cap-acute coronary syndrome, NGAL: neutrophil-gelatinase associated lipocalin;Own illustration modified from the original publication: Meteva et al., EHJ, 2023, doi: 10.1093/eurheartj/ehad379*

We additionally observed a strong band expression at 130kDa corresponding to the MMP9/NGAL (neutrophil gelatinase-associated lipocalin) heterodimer, a complex known to preserve MMP9 from degradation and thereby extending its function (29).

We additionally observed an increased local gelatinolytic activity only in IFC-ACS plasma samples as compared to RFC-ACS (figure 11), underlining again the distinct local activation of MMP9 in the pathology of plaque erosion.

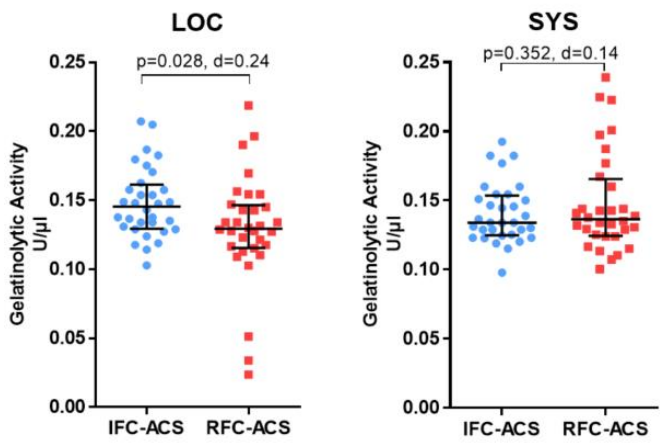

Figure 11: Increased local MMP9 activity in plasma samples from IFC-ACS vs. RFC-ACS patients; *d < 0.2 small effect, d between 0.2 and 0.8 medium effect, d > 0.8 large effect; Abbreviations: LOC: local, SYS: systemic, RFC-ACS: ruptured fibrous cap acute coronary syndrome, IFC-ACS: intact fibrous cap-acute coronary syndrome;*

Own illustration modified from the original publication: Meteva et al., EHJ, 2023, doi: 10.1093/eurheartj/ehad379

Furthermore, we unravelled a complex synergy between local MMP9 activation and disturbed flow conditions leading to the hall mark of plaque erosion: the local detachment of endothelial cells from the surface of the plaque. An in-vitro experiment imitating different flow conditions (laminar vs. oscillatory) on an endothelial cell monolayer, showed that both factors: turbulent flow and activated MMP9 are required in order to induce significant detachment of endothelial cells (figure 12).

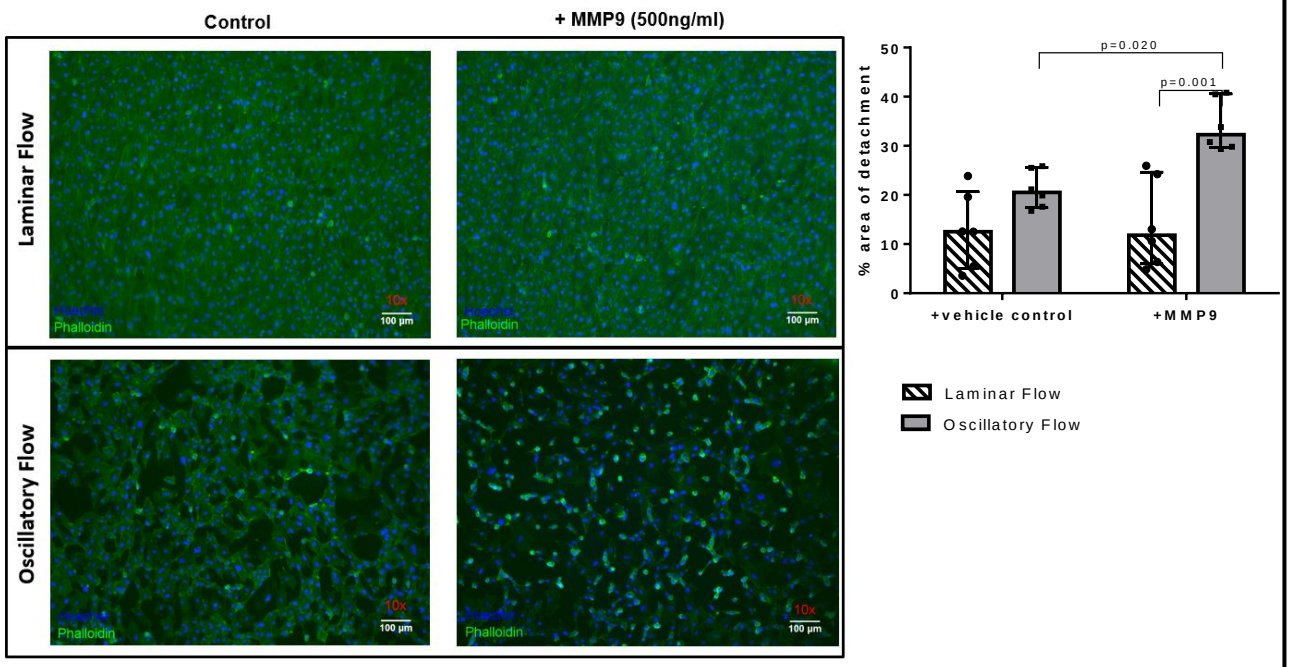

Figure 12: A representative histological image showing significant detachment of endothelial cells only under the combination of both factors: oscillatory flow and MMP9. *Abbreviations/Legend: MMP9: matrix metalloproteinase 9, Hoechst: DNA stain showing nuclei in blue; Phalloidin: F-Actin staining in green; Own illustration modified from the original publication: Meteva et al., EHJ, 2023, doi: 10.1093/eurheartj/ehad379*

4.4. The Effect of TLR2 Activation on Neutrophil Survival and Cytotoxicity

A TLR2 activation of local IFC-ACS derived neutrophils led to an increased survival with lower shedding of CD16 (lower CD16lo/CD16hi ratio) as an indirect marker of apoptosis (figure 13A). This effect was not evident in local RFC-ACS neutrophils (figure 13A).

IFC-ACS- derived neutrophils also exhibited higher cytotoxicity in a co-culture experiment with endothelial cells independently of TLR2, leading to increased endothelial cell death as a complementary mechanism of endothelial cell detachment in IFC-ACS (figure 13B).

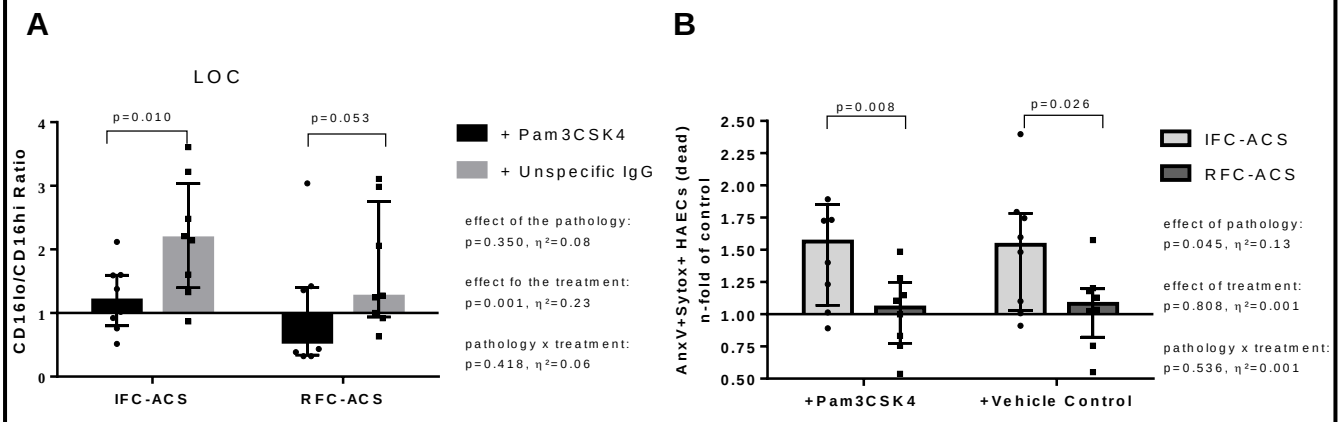

Figure 13: A) Increased neutrophil survival in local IFC-ACS derived neutrophils B)Higher neutrophil-induced endothelial cell death regardless of TLR2-treatment in IFC-ACS vs. RFC-ACS; *small effect η^2<0.01, medium effect η^2 between 0.01 and 0.14, large effect η^2 >0.14; Abbreviations: RFC-ACS: ruptured fibrous cap acute coronary syndrome; IFC-ACS: intact fibrous cap-acute coronary syndrome; HAECs: human aortic endothelial cells; Pam3CSK4: synthetic TLR2/1-agonist; Own illustration modified from the original publication: Meteva et al., EHJ, 2023, doi: 10.1093/eurheartj/ehad379*

4.5. Endogenous TLR2 Activation through Hyaluronan in Plaque Erosion

Histological analysis of thrombus specimen of eroded plaques showed increased expression of hyaluronidase 2 (HYAL2): an enzyme, capable of cleaving hyaluronan into its pro-inflammatory form of low-molecular hyaluronan, which is a known agonist of the TLR2 receptor (6, 30, 31) (figure 14A). Correspondingly, the local plasma concentration of hyaluronan (HA) was increased in IFC-ACS vs. RFC-ACS complementing the TLR2-activation cascade (figure 14B).

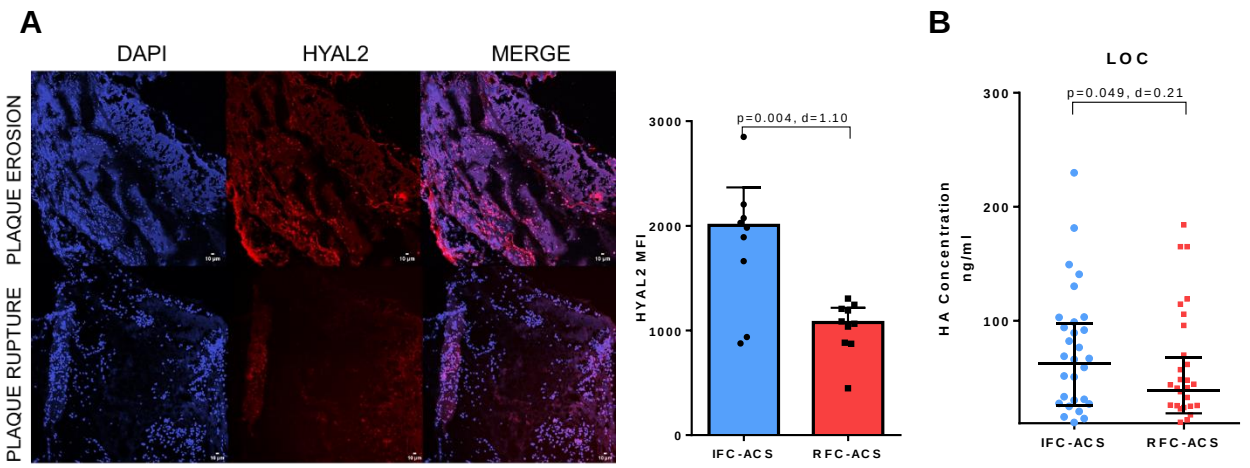

Figure 14: A) Representative immunohistochemical thrombus staining showing an increased HYAL2 expression on the outer part of the thrombus in plaque erosion; B) Increased local HA plasma concentrations in IFC-ACS; *d < 0.2 small effect, d between 0.2 and 0.8 medium effect, d > 0.8 large effect; Abbreviations: HA: hyaluronic acid; HYAL2: hyaluronidase 2; MFI: median fluorescence intensity; LOC: local; RFC-ACS: ruptured fibrous cap acute coronary syndrome; IFC-ACS: intact fibrous cap-acute coronary syndrome; DAPI: nucleus staining;* *Own illustration modified from the original publication: Meteva et al., EHJ, 2023, doi: 10.1093/eurheartj/ehad379*

5. Discussion

5.1 Summary of the Results

The OPTICO-ACS study aimed to characterize two different pathophysiologies of acute coronary syndrome: the well-known ‘plaque rupture’ and the less understood ‘plaque erosion’ as the second most common pathophysiology of ACS. Furthermore, our recent studies showed distinct immunological signatures and different clinical outcomes between both pathophysiologies of ACS, with more favourable outcome for patients with plaque erosion than plaque rupture(32). So, the current study advances this knowledge, unravelling a complementary novel mechanism of TLR2-driven activation of neutrophil granulocytes at the culprit lesion site of ACS with intact fibrous cap, also known as plaque erosion.

Despite equal distribution, local neutrophils from the coronary environment in plaque erosion show a higher susceptibility to TLR2-activation in comparison to systemic erosion-derived or rupture-derived neutrophils in general, underlining a very specific immunological pattern at the coronary lesion site of plaque erosion. Upon TLR2-stimulation, local IFC-ACS-derived neutrophils produce higher amounts of active MMP9 (33), a gelatinase capable of degrading the extracellular matrix on which endothelial cells adhere and thereby promoting desquamation of endothelial cells as a hallmark of plaque erosion (7, 33). Nevertheless, a second hit in addition to MMP9 is required for endothelial cell detachment: turbulent flow, which points towards a specific mechanism localized at coronary bifurcations as the pre-disposition areas of plaque erosion (2, 18, 34). Furthermore, TLR2-activation of local IFC-ACS-derived neutrophils led to enhanced neutrophils survival (33). In this context, thrombus specimens from erosion patients exhibited higher amounts of hyaluronidase 2, an enzyme capable of delivering significant amounts of the pro-inflammatory form of the endogenous TLR2-activator: hyaluronan, which concentration was remarkably higher in the local IFC-ACS plasma samples (33). Finally, we observed enhanced neutrophil cytotoxicity towards endothelial cells in patients with plaque erosion than plaque rupture, indicating the crucial direct contribution of the neutrophils to the pathophysiology of IFC-ACS (33).

5.2 Interpretation of the Results in the Context of the current Research

The current results arise from a prospective multicentre clinical study aiming to characterize the immune activation in patients with plaque erosion and plaque rupture and thereby providing high research quality in a translational setting, allowing a better integration of the results in the disease context. The results also point toward a new specific mechanism of neutrophil activation at the coronary lesion site of plaque erosion, allowing for identification of future therapeutic targets.

The neutrophil granulocytes have always been the subject of vast scientific interest in the atherosclerosis research as their infiltration in vulnerable plaques has been associated to features of plaque destabilization and subsequent coronary thrombosis (3, 17, 35). However, the current study shows that not only infiltrating neutrophils may be capable of active contribution to plaque vulnerability, but also blood neutrophils, which show different phenotypes and receptor repertoire in dependence of the underlying ACS-pathophysiology. Thereby, the current study indicates a distinct neutrophil phenotype in plaque erosion, localized in the bloodstream at the coronary culprit lesion site.

Some studies, concentrated on the association between a high neutrophil count and mortality prediction in acute coronary syndrome and other diseases like diabetes (36, 37). However, our study emphasizes a different neutrophil functionality despite of equal cell count as more important in the pathophysiology of acute coronary syndrome with intact fibrous cap.

In this regard, the TLR2-activation on endothelial cells in combination with high shear stress and the subsequent secondary neutrophil adherence have been previously shown as important contributors to plaque erosion, whereby the neutrophil adherence to the activated endothelium only aggravated the cascade (6). However, in contrast to Quillard et al. our translational study indicates a main contributory role of the neutrophils and their TLR2 activation to the subsequent endothelial detachment and cytotoxicity, underlining again the multifaceted pathophysiology of plaque erosion.

Furthermore, through the TLR2-dependant MMP9 production neutrophils from IFC-ACS patients may polarise T-cells through the cleavage of CD31 and thereby lead to T-cell

dysregulation: a very important complementary pathophysiological mechanism in NSTE-ACS (38). Supporting this hypothesis, our study showed indirect evidence of higher soluble CD31 levels in local IFC-ACS plasma samples, suggesting a similar cross-talk mechanism between neutrophils and T cells in plaque erosion (33).

Neutrophils are the first immune cells to arrive at sites of inflammation and to orchestrate the further inflammatory cascade(7), therefore we consider the TLR2-dependent neutrophil activation in plaque erosion as extremely important initiator of the distinct T cell immune response, that we observed in our previous studies (19).

In conclusion, our results advance the understanding of the complex pathophysiology of plaque erosion, involving innate and adaptive immune activation pathways (19, 33) and thereby emphasizing the importance of the cross-talk between different immune cell populations (39).

5.3 Strengths and Limitations of the Study

One of the main strengths of the current study is the translational design, giving access to human blood samples and clinical information in order to achieve deep characterization of the pathophysiological mechanisms involved in these particular disease entities. Besides, the study has a blinded unbiased design, so the performer of the in-vitro experiments was unaware of the underlying pathophysiology until the end of the study. Furthermore, through the multicentre study design a certain scientific quality standard is being guaranteed, as for example the OCT imaging was simultaneously assessed by two independent core labs allowing for high quality of analysis and an unbiased diagnosis of erosion or rupture. In this context the histological analysis of the thrombus specimens was performed in our collaboration laboratory in the university department of cardiology in Rome, allowing again for external validation of results.

One of the main limitations of the study is surely the lack of information on the patients and their immune activity before the acute coronary syndrome as the inclusion in the study was only possible at the time of the index event, so we can only make associations, but not deduce causality for the time before the event. Furthermore, we lack information

on the chronic immune activation state after the ACS event, so a future personalised therapeutic approach would require this type of information as well.

The matching strategy applied in the study may control for some known variables to affect the neutrophil activation, but a residual confounding still remains.

In the current study, we use isolated human neutrophils for the in-vitro experiments and thereby separate the neutrophils from other immune cells and their soluble metabolites, present at the site of the culprit lesion, which may to some extent manipulate the immune response to the TLR2-activation. In this context, by using Pam3CSK4 as a synthetic TLR2 agonist, we address only the TLR2/TLR1 heterodimer, even though TLR2 can build heterodimers with TLR6 as well, which should be taken into consideration when interpreting the results in detail. Nevertheless, the two signalling pathways show great similarities, and therefore the current approach should not affect the results significantly (40).

5.4 Implications for future Research Goals

Plaque erosion is a unique ACS-causing pathophysiology characterized by a distinct inflammatory signature marked by the activation of neutrophils and T cells (19, 32, 33). In this context, the establishment of personalized future therapeutic targets for this particular disease population is one of the main aims of the future cardiovascular research. Currently, we describe a novel neutrophil activation pathway, dominated by TLR2, turbulent flow conditions and the release of hyaluronan as an endogenous activator of the TLR2-cascade. In this context, a temporary anti-inflammatory treatment in plaque erosion targeted at TLR2 seem to depict a plausible future therapeutic aim and requires further scientific validation. Importantly, a deep characterization of the chronic neutrophil response after plaque erosion is one of the main future research focuses in order to develop a personalized precisely timed therapeutic anti-TLR2 approach with negligible side effects. A further very important aspect to a better understanding of the endogenous TLR2 activation in plaque erosion is a broad proteomics analysis of novel potential TLR2 agonists apart from hyaluronan, as the current study lack information on further possible modifiable ligands. Furthermore, a deeper, more precise characterization of the interplay between neutrophils and T cells may open the door to an entirely new immunomodulatory strategies.

6. Conclusion

In summary, the current translational study provides novel insights into the complex, multifactor pathology of plaque erosion, characterized by a distinct TLR2-driven neutrophil response under turbulent flow conditions with a subsequent MMP9 release and detachment of endothelial cells as the hallmark of plaque erosion. Furthermore, a higher endogenous release of hyaluronan may trigger and enhance the TLR2-activation cascade. Future studies are required for a deeper understanding of the therapeutic potential of the current findings in the era of personalized medicine.

References

1. Yamamoto E, Yonetsu T, Kakuta T, Soeda T, Saito Y, Yan BP, Kurihara O, Takano M, Niccoli G, Higuma T, Kimura S, Minami Y, Ako J, Adriaenssens T, Boeder NF, Nef HM, Fracassi F, Sugiyama T, Lee H, Crea F, Kimura T, Fujimoto JG, Fuster V, Jang IK. Clinical and Laboratory Predictors for Plaque Erosion in Patients With Acute Coronary Syndromes. J Am Heart Assoc. 2019;8(21):e012322.
2. Libby P, Pasterkamp G. Requiem for the 'vulnerable plaque'. Eur Heart J. 2015;36(43):2984-7.
3. Virmani R, Burke AP, Farb A, Kolodgie FD. Pathology of the vulnerable plaque. J Am Coll Cardiol. 2006;47(8 Suppl):C13-8.
4. Libby P. Inflammation in atherosclerosis. Nature. 2002;420(6917):868-74.
5. Leistner DM, Krankel N, Meteva D, Abdelwahed YS, Seppelt C, Stahli BE, Rai H, Skurk C, Lauten A, Mochmann HC, Frohlich G, Rauch-Krohnert U, Flores E, Riedel M, Sieronski L, Kia S, Strassler E, Haghikia A, Dirks F, Steiner JK, Mueller DN, Volk HD, Klotsche J, Joner M, Libby P, Landmesser U. Differential immunological signature at the culprit site distinguishes acute coronary syndrome with intact from acute coronary syndrome with ruptured fibrous cap: results from the prospective translational OPTICO-ACS study. Eur Heart J. 2020;41(37):3549-60.
6. Quillard T, Araujo HA, Franck G, Shvartz E, Sukhova G, Libby P. TLR2 and neutrophils potentiate endothelial stress, apoptosis and detachment: implications for superficial erosion. Eur Heart J. 2015;36(22):1394-404.
7. Libby P, Pasterkamp G, Crea F, Jang IK. Reassessing the Mechanisms of Acute Coronary Syndromes. Circ Res. 2019;124(1):150-60.
8. Scheibner KA, Lutz MA, Boodoo S, Fenton MJ, Powell JD, Horton MR. Hyaluronan fragments act as an endogenous danger signal by engaging TLR2. J Immunol. 2006;177(2):1272-81.
9. Vinci R, Pedicino D, D'Aiello A, Ciampi P, Ponzo M, Bonanni A, Russo G, Montone RA, Massetti M, Crea F, Liuzzo G. Platelet hyaluronidase 2 enrichment in acute coronary syndromes: a conceivable role in monocyte-platelet aggregate formation. J Enzym Inhib Med Ch. 2021;36(1):785-9.
10. Pedicino D, Vinci R, Giglio AF, Pisano E, Porto I, Vergallo R, Russo G, Ruggio A, D'Aiello A, Flego D, Annibali G, Trotta F, Piacentini R, Niccoli G, Liuzzo G, Crea F. Alterations of Hyaluronan Metabolism in Acute Coronary Syndrome. J Am Coll Cardiol. 2018;72(13):1490-503.
11. Kolte D, Yonetsu T, Ye JC, Libby P, Fuster V, Jang IK. Optical Coherence Tomography of Plaque Erosion: JACC Focus Seminar Part 2/3. J Am Coll Cardiol. 2021;78(12):1266-74.
12. van der Wal AC, Becker AE, van der Loos CM, Das PK. Site of intimal rupture or erosion of thrombosed coronary atherosclerotic plaques is characterized by an inflammatory process irrespective of the dominant plaque morphology. Circulation. 1994;89(1):36-44.
13. Arbustini E, Dal Bello B, Morbini P, Burke AP, Bocciarelli M, Specchia G, Virmani R. Plaque erosion is a major substrate for coronary thrombosis in acute myocardial infarction. Heart. 1999;82(3):269-72.
14. Yonetsu T, Lee T, Murai T, Suzuki M, Matsumura A, Hashimoto Y, Kakuta T. Plaque morphologies and the clinical prognosis of acute coronary syndrome caused by lesions with intact fibrous cap diagnosed by optical coherence tomography. Int J Cardiol. 2016;203:766-74.

15. Jia HB, Abtahian F, Aguirre AD, Lee S, Chia S, Lowe H, Kato KJ, Yonetsu T, Vergallo R, Hu SN, Tian JW, Lee H, Park SJ, Jang YS, Raffel OC, Mizuno K, Uemura S, Itoh T, Kakuta T, Choi SY, Dauerman HL, Prasad A, Toma C, McNulty I, Zhang S, Yu B, Fuster V, Narula J, Virmani R, Jang IK. In Vivo Diagnosis of Plaque Erosion and Calcified Nodule in Patients With Acute Coronary Syndrome by Intravascular Optical Coherence Tomography. J Am Coll Cardiol. 2013;62(19):1748-58.
16. Seegers LM, Araki M, Nakajima A, Yonetsu T, Minami Y, Ako J, Soeda T, Kurihara O, Higuma T, Kimura S, Adriaenssens T, Nef HM, Lee H, McNulty I, Sugiyama T, Kakuta T, Jang IK. Sex Differences in Culprit Plaque Characteristics Among Different Age Groups in Patients With Acute Coronary Syndromes. Circ Cardiovasc Interv. 2022;15(6):e011612.
17. Bentzon JF, Otsuka F, Virmani R, Falk E. Mechanisms of Plaque Formation and Rupture. Circulation Research. 2014;114(12):1852-66.
18. McElroy M, Kim Y, Niccoli G, Vergallo R, Langford-Smith A, Crea F, Gijsen F, Johnson T, Keshmiri A, White SJ. Identification of the haemodynamic environment permissive for plaque erosion. Sci Rep. 2021;11(1):7253.
19. Leistner DM, Kränkel N, Meteva D, Abdelwahed YS, Seppelt C, Stähli BE, Rai H, Skurk C, Lauten A, Mochmann H-C, Fröhlich G, Rauch-Kröhnert U, Flores E, Riedel M, Sieronski L, Kia S, Strässler E, Haghikia A, Dirks F, Steiner JK, Mueller DN, Volk H-D, Klotsche J, Joner M, Libby P, Landmesser U. Differential immunological signature at the culprit site distinguishes acute coronary syndrome with intact from acute coronary syndrome with ruptured fibrous cap: results from the prospective translational OPTICO-ACS study. Eur Heart J. 2020;41(37):3549-60.
20. Rosales C. Neutrophil: A Cell with Many Roles in Inflammation or Several Cell Types? Front Physiol. 2018;9.
21. Gupta AK, Joshi MB, Philippova M, Erne P, Hasler P, Hahn S, Resink TJ. Activated endothelial cells induce neutrophil extracellular traps and are susceptible to NETosis-mediated cell death. Febs Lett. 2010;584(14):3193-7.
22. Simmons SR, Tchalla EYI, Bhalla M, Ghanem ENB. The Age-Driven Decline in Neutrophil Function Contributes to the Reduced Efficacy of the Pneumococcal Conjugate Vaccine in Old Hosts. Frontiers in Cellular and Infection Microbiology. 2022;12.
23. Zhang DC, Chen G, Manwani D, Mortha A, Xu CL, Faith JJ, Burk RD, Kunisaki Y, Jang JE, Scheiermann C, Merad M, Frenette PS. Neutrophil ageing is regulated by the microbiome. Nature. 2015;525(7570):528-+.
24. Tanji-Matsuba K, van Eeden SF, Saito Y, Okazawa M, Klut ME, Hayashi S, Hogg JC. Functional changes in aging polymorphonuclear leukocytes. Circulation. 1998;97(1):91-8.
25. Spitzer JA. Gender differences in some host defense mechanisms. Lupus. 1999;8(5):380-3.
26. Wong SL, Demers M, Martinod K, Gallant M, Wang Y, Goldfine AB, Kahn CR, Wagner DD. Diabetes primes neutrophils to undergo NETosis, which impairs wound healing. Nat Med. 2015;21(7):815-9.
27. Dransfield I, Buckle AM, Savill JS, Mcdowall A, Haslett C, Hogg N. Neutrophil Apoptosis Is Associated with a Reduction in Cd16 (Fc-Gamma-Riii) Expression. Journal of Immunology. 1994;153(3):1254-63.
28. Niven DJ, Berthiaume LR, Fick GH, Laupland KB. Matched case-control studies: a review of reported statistical methodology. Clin Epidemiol. 2012;4:99-110.
29. Bouchet S, Bauvois B. Neutrophil Gelatinase-Associated Lipocalin (NGAL), Pro-Matrix Metalloproteinase-9 (pro-MMP-9) and Their Complex Pro-MMP-9/NGAL in Leukaemias. Cancers (Basel). 2014;6(2):796-812.

30. Cowman MK, Lee HG, Schwertfeger KL, McCarthy JB, Turley EA. The content and size of hyaluronan in biological fluids and tissues. Frontiers in Immunology. 2015;6.
31. Cyphert JM, Trempus CS, Garantziotis S. Size Matters: Molecular Weight Specificity of Hyaluronan Effects in Cell Biology. International Journal of Cell Biology. 2015;2015:563818.
32. Gerhardt T, Seppelt C, Abdelwahed YS, Meteva D, Wolfram C, Stapmanns P, Erbay A, Zanders L, Nelles G, Musfeld J, Sieronski L, Stahli BE, Montone RA, Vergallo R, Haghikia A, Skurk C, Knebel F, Dreger H, Trippel TD, Rai H, Joner M, Klotsche J, Libby P, Crea F, Krankel N, Landmesser U, Leistner DM, group O-As. Culprit plaque morphology determines inflammatory risk and clinical outcomes in acute coronary syndrome. Eur Heart J. 2023.
33. Meteva D, Vinci R, Seppelt C, Abdelwahed YS, Pedicino D, Nelles G, Skurk C, Haghikia A, Rauch-Krohnert U, Gerhardt T, Straessler E, Zhao Y, Golla F, Joner M, Rai H, Kratzer A, Arnal HG, Liuzzo G, Klotsche J, Crea F, Landmesser U, Leistner DM, Krankel N. Toll-like receptor 2, hyaluronan, and neutrophils play a key role in plaque erosion: the OPTICO-ACS study. Eur Heart J. 2023.
34. Yamamoto E, Thondapu V, Poon E, Sugiyama T, Fracassi F, Dijkstra J, Lee H, Ooi A, Barlis P, Jang IK. Endothelial Shear Stress and Plaque Erosion: A Computational Fluid Dynamics and Optical Coherence Tomography Study. JACC Cardiovasc Imaging. 2019;12(2):374-5.
35. Mortaz E, Alipoor SD, Adcock IM, Mumby S, Koenderman L. Update on Neutrophil Function in Severe Inflammation. Front Immunol. 2018;9:2171.
36. Ji ZJ, Liu GR, Guo JQ, Zhang R, Su YM, Carvalho A, Qu YY, Zuo WJ, Yao YY, Lin J, Ma GS. The Neutrophil-to-Lymphocyte Ratio Is an Important Indicator Predicting In-Hospital Death in AMI Patients. Front Cardiovasc Med. 2021;8.
37. Woo SJ, Ahn SJ, Ahn J, Park KH, Lee K. Elevated Systemic Neutrophil Count in Diabetic Retinopathy and Diabetes: A Hospital-Based Cross-sectional Study of 30,793 Korean Subjects. Invest Ophth Vis Sci. 2011;52(10):7697-703.
38. Angelini G, Flego D, Vinci R, Pedicino D, Trotta F, Ruggio A, Piemontese GP, Galante D, Ponzo M, Biasucci LM, Liuzzo G, Crea F. Matrix metalloproteinase-9 might affect adaptive immunity in non-ST segment elevation acute coronary syndromes by increasing CD31 cleavage on CD4+T-cells. Eur Heart J. 2018;39(13):1089-97.
39. Costa S, Bevilacqua D, Cassatella MA, Scapini P. Recent advances on the crosstalk between neutrophils and B or T lymphocytes. Immunology. 2019;156(1):23-32.
40. Farhat K, Riekenberg S, Heine H, Debarry J, Lang R, Mages J, Buwitt-Beckmann U, Roeschmann K, Jung G, Wiesmuller KH, Ulmer AJ. Heterodimerization of TLR2 with TLR1 or TLR6 expands the ligand spectrum but does not lead to differential signaling. J Leukocyte Biol. 2008;83(3):692-701.

Statutory Declaration

“I, **Denitsa Meteva**, by personally signing this document in lieu of an oath, hereby affirm that I prepared the submitted dissertation on the topic: *Die pathophysiologische Rolle der Toll-like Rezeptor 2 Aktivierung in den neutrophilen Granulozyten in Patienten mit Akutem Koronarsyndrom mit intakter oder rupturierter fibröser Kappe/ The Pathophysiological Role of Toll-like Receptor 2 Activation in Neutrophil Granulocytes in Patients with Acute Coronary Syndrome with Intact vs. Ruptured Fibrous Cap* independently and without the support of third parties, and that I used no other sources and aids than those stated.

All parts which are based on the publications or presentations of other authors, either in letter or in spirit, are specified as such in accordance with the citing guidelines. The sections on methodology (in particular regarding practical work, laboratory regulations, statistical processing) and results (in particular regarding figures, charts and tables) are exclusively my responsibility. Furthermore, I declare that I have correctly marked all of the data, the analyses, and the conclusions generated from data obtained in collaboration with other persons, and that I have correctly marked my own contribution and the contributions of other persons (cf. declaration of contribution). I have correctly marked all texts or parts of texts that were generated in collaboration with other persons. My contributions to any publications to this dissertation correspond to those stated in the below joint declaration made together with the supervisor. All publications created within the scope of the dissertation comply with the guidelines of the ICMJE (International Committee of Medical Journal Editors; www.icmje.org) on authorship. In addition, I declare that I shall comply with the regulations of Charité – Universitätsmedizin Berlin on ensuring good scientific practice. I declare that I have not yet submitted this dissertation in identical or similar form to another Faculty.

The significance of this statutory declaration and the consequences of a false statutory declaration under criminal law (Sections 156, 161 of the German Criminal Code) are known to me.”

_____ _____

Date Signature

Declaration of contribution to the publication

Denitsa Meteva contributed the following to the below listed publication:

Publication 1: Denitsa Meteva, Ramona Vinci, Claudio Seppelt, Youssef S Abdelwahed, Daniela Pedicino, Gregor Nelles, Carsten Skurk, Arash Haghikia, Ursula Rauch-Kröhnert, Teresa Gerhardt, Elisabeth Straessler, Yingjie Zhao, Felix Golla, Michael Joner, Himanshu Rai, Adelheid Kratzer, Hector Giral Arnal, Giovanna Liuzzo, Jens Klotsche, Filippo Crea, Ulf Landmesser, David M Leistner, Nicolle Kränkel, **Toll-like receptor 2, hyaluronan, and neutrophils play a key role in plaque erosion: the OPTICO–ACS study**, European Heart Journal, Volume 44, Issue 38, 7 October 2023, Pages 3892–3907, https://doi.org/10.1093/eurheartj/ehad379

Contribution:

The doctoral student is the **only first author** of the publication. She had the leading role in the generation of the hypothesis, the planning and design of the experiments, as well as in their performance, troubleshooting and analysis. The doctoral candidate performed **all of the experiments,** analysed **the whole data set according to the study protocol (for the immunohistochemical thrombus analysis in collaboration with the Dr. R. Vinci from the University of Rome)** and created **all figures, all graphs and all tables herself**. The doctoral candidate **wrote the whole manuscript (abstract, introduction, methods, results and discussion)** and **was responsible for the entire peer review and revision process during the manuscript submission**. The whole data analysis behind each figure and table was initially performed by the doctoral student and afterwards verified by the study statistician. The doctoral student responded to the comments of the reviewers to their fullest satisfaction and revised herself the manuscript accordingly. The quality of the work of the doctoral student was constantly ensured by the first supervisor through scientific guidance and verification.

_____

Signature, date and stamp of first supervising university professor / lecturer

_____

Signature of doctoral candidate

Print Copy of the Publication

ESC European Society of Cardiology

European Heart Journal (2023) **44**, 3892–3907
https://doi.org/10.1093/eurheartj/ehad379

TRANSLATIONAL RESEARCH
Vascular biology and medicine

Toll-like receptor 2, hyaluronan, and neutrophils play a key role in plaque erosion: the OPTICO–ACS study

Denitsa Meteva [1,2,3]*, Ramona Vinci [9,10], Claudio Seppelt [1,2,3,12], Youssef S. Abdelwahed[1,2,3], Daniela Pedicino[9,10], Gregor Nelles[1,2], Carsten Skurk [1,2,3], Arash Haghikia [1,2,3,4], Ursula Rauch-Kröhnert[1,2,3], Teresa Gerhardt [1,2,3,4], Elisabeth Straessler[1,2,3], Yingjie Zhao[1,2], Felix Golla[1,2], Michael Joner [5,6], Himanshu Rai [7,8], Adelheid Kratzer[1,2,3], Hector Giral Arnal[1,2,3], Giovanna Liuzzo[9,10], Jens Klotsche[2,11], Filippo Crea [9,10], Ulf Landmesser [1,2,3,4]†, David M. Leistner[1,2,3,4,12]†, and Nicolle Kränkel [1,2,3]†

[1]Deutsches Herzzentrum der Charité, Department of Cardiology, Angiology and Intensive Care Medicine, Hindenburgdamm 30, Berlin 12203, Germany; [2]Charité—Universitätsmedizin Berlin, Corporate member of Freie Universität Berlin and Humboldt-Universität zu Berlin, Charitéplatz 1, Berlin 10117, Germany; [3]DZHK (German Centre for Cardiovascular Research) partner Site Berlin, Berlin 12203, Germany; [4]Berlin Institute of Health (BIH), Anna-Louisa-Karsch-Str. 2, Berlin 10178, Germany; [5]Department of Cardiology and ISAR Research Centre, German Heart Centre Munich, Lazarettstrasse 36, Munich 80636, Germany; [6]DZHK (German Centre for Cardiovascular Research) partner Site Munich, Munich 80636, Germany; [7]Cardiovascular Research Institute Dublin, Mater Private Network, 73 Eccles Street, Dublin D07 YH66, Ireland; [8]School of Pharmacy and Biomolecular Sciences, RCSI University of Medicine and Health Sciences, 123 St. Stephan's Green, Dublin D02 YN77, Ireland; [9]Department of Cardiovascular and Pulmonary Sciences, Catholic University of the Sacred Heart, Largo Francesco Vito 1, Rome 00168, Italy; [10]Department of Cardiovascular Sciences, IRCCS Fondazione Policlinico Universitario A. Gemelli, Largo Francesco Vito 1, Rome 00168, Italy; [11]German Rheumatism Research Centre (DRFZ) and Institute for Social Medicine, Epidemiology and Health Economy, Charité University Medicine Berlin, Campus Charite Mitte, Charitéplatz 1, Berlin 10117, Germany; and [12]Department of Cardiology and Angiology, Goethe University, Theodor-Stern-Kai 7, Frankfurt am Main 60598, Germany

Received 1 September 2022; revised 15 May 2023; accepted 25 May 2023; online publish-ahead-of-print 30 June 2023

See the editorial comment for this article 'Unravelling the heart's comic drama: can TLRs and hyaluronan metabolism stoke neutrophil rage in acute coronary syndrome?', by G. Franck, https://doi.org/10.1093/eurheartj/ehad455.

Abstract

Background and aims In one-third of patients with acute coronary syndrome (ACS), thrombosis occurs despite an intact fibrous cap (IFC) (IFC–ACS, 'plaque erosion'). Recent studies emphasize neutrophils as the immediate inflammatory response in this pathology, but their exact molecular activation patterns are still poorly understood and may represent future therapeutic targets.

Methods and results Thirty-two patients with IFC–ACS and matched patients with ACS with ruptured fibrous cap (RFC) (RFC–ACS) from the OPTICO–ACS study were included, and blood samples were collected from the local site of the culprit lesion and the systemic circulation. Neutrophil surface marker expression was quantified by flow cytometry. Neutrophil cytotoxicity towards endothelial cells was examined in an *ex vivo* co-culture assay. Secretion of active matrix metalloproteinase 9 (MMP9) by neutrophils was evaluated using zymography in supernatants and in plasma samples. Optical coherence tomography (OCT)–embedded thrombi were used for immunofluorescence analysis. Toll-like receptor 2 (TLR2) expression was higher on neutrophils from IFC–ACS than RFC–ACS patients. TLR2 stimulation increased the release of active MMP9 from local IFC–ACS–derived neutrophils, which also aggravated endothelial cell death independently of TLR2. Thrombi of IFC–ACS patients exhibited more hyaluronidase 2 with concomitant increase in local plasma levels of the TLR2 ligand: hyaluronic acid.

Conclusion The current study provides first in-human evidence for distinct TLR2-mediated neutrophil activation in IFC–ACS, presumably triggered by elevated soluble hyaluronic acid. Together with disturbed flow conditions, neutrophil-released MMP9 might be promoting endothelial cell loss–triggered thrombosis and therefore providing a potential future target for a phenotype-specific secondary therapeutic approach in IFC–ACS.

* Corresponding author. Tel: +49 30 450 654 087, Fax: +49 30 450 513 999, Email: denitsa.meteva@dhzc-charite.de
† These authors contributed equally to this work.

Structured Graphical Abstract

Key Question

The exact pathophysiological mechanisms of acute coronary syndrome with intact fibrous cap (IFC-ACS), also known as 'plaque erosion', remain incompletely understood. Therefore, this study aims to characterize the neutrophil activation patterns in the well-characterized patient cohort of the OPTICO-ACS study.

Key Finding

Local toll-like receptor 2 (TLR2)-dependant neutrophil activation, presumably driven by disturbed blood flow, higher expression of hyaluronidase 2 (HYAL2) and increased local concentration of hyaluronic acid (HA), aggravated neutrophil-mediated endothelial cell death and release of activated matrix metalloproteinase 9 (MMP9).

Take Home Message

Increased TLR2-expression and local TLR2-activation by HA may lead to neutrophil dysregulation, which in combination with disturbed flow conditions triggers MMP9-release and thereby aggravates endothelial cell detachment and potentially T-cell mediated cytotoxicity in patients with IFC-ACS. MMP9 may also contribute to T-cell dysregulation due to CD31 cleavage as shown by other studies.

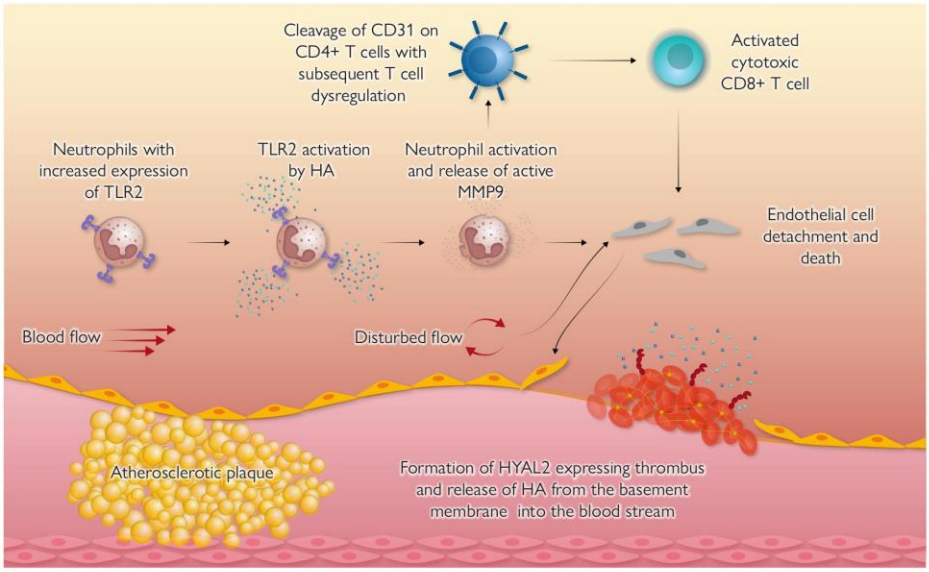

TLR2, Toll-like receptor 2; HA, hyaluronic acid; MMP9, matrix metalloproteinase 9; HYAL2, hyaluronidase 2.

Keywords Plaque erosion • Neutrophils • Hyaluronic acid • Toll-like receptor 2 • Matrix metalloproteinase 9 • Endothelial cell death

Translational perspective

The functional characterization of neutrophils from the coronary lesion site of patients with ACS provides mechanistic insights into the immunovascular processes in different ACS phenotypes. The enhanced TLR2 response of local IFC–ACS–derived neutrophils, resulting in MMP9 release and endothelial cell detachment, implicates possible future therapeutic targets and prevention strategies specifically in this ACS entity.

Introduction

Ischemic heart disease and its most dramatic manifestation acute coronary syndrome (ACS) remain the leading cause of death worldwide, despite effective lipid lowering therapies.[1,2] Extensive effort has been made over the past decades to better characterize the molecular pathomechanisms of ACS, in order to predict and minimize cardiovascular event burden.[2]

These investigations have mainly focused on the mechanisms of rupture of the fibrous cap covering the plaque,[3] the most frequent

phenotype of ACS.[4,5] However, autopsy studies have suggested another mechanism of ACS, i.e. coronary plaque erosion, characterized by thrombus formation on a plaque with intact fibrous cap (IFC) and, compared with ruptured fibrous cap (RFC) plaques, less lipid accumulation and local endothelial injury with loss of the luminal endothelial layer on the surface of the plaque.[4] Contemporary intravascular imaging studies using optical coherence tomography (OCT) implicate IFC in up to one-third of ACS cases.[6] However, the underlying pathophysiological mechanisms of IFC–ACS remain incompletely understood. Few ACS studies observed macrophage infiltrations at eroded ACS–causing sites and thereby suggest that inflammatory mechanisms may play a crucial role in this pathology.[7,8,9] Notably, the neutrophils are shown to be the first immune cells to arrive at ACS–causing culprit sites and are thereby considered to be key initiators of the following inflammatory cascade after myocardial infarction.[10] Neutrophil accumulation, disturbed flow, and engagement of the endothelial TLR2 receptor have been previously suggested to aggravate endothelial cell detachment in an *in vitro* model of plaque erosion.[11] Therefore, this study aimed to characterize the mechanisms behind the neutrophil activation in patients with IFC–ACS with a special focus on neutrophil TLR2 activation.

Materials and methods

Study design

The current sub-study of the observational, prospective OPTICO–ACS study program enrolled patients with non-ST elevation myocardial infarction[12] or ST elevation myocardial infarction[13] and undergoing OCT imaging of the ACS–causing culprit lesion according to the inclusion and exclusion criteria.[8] The OPTICO–ACS study was designed not only to assess the rates of major adverse cardiovascular events in patients with IFC–ACS vs. RFC–ACS as a primary endpoint but also to characterize these two populations by a combination of clinical description, OCT imaging of the culprit lesion, and immunophenotyping using flow cytometry.[8]

In the current nested case–control sub-study, 32 patients with IFC–ACS were matched by known factors to affect the neutrophil activation: age (±5 years),[14–16] biological sex,[17] and diabetes mellitus type 2[18] to patients with RFC–ACS (see Supplementary data online, *Material S1*). On the variables 'sex' and 'diabetes mellitus type 2', we performed an exact matching strategy (one to one), whereby on 'age', we performed an individual matching with a range of ±5 years. If more than one matched RFC–ACS control was available, the patient with the closest age to the matched IFC–ACS patient was randomly selected. The study was approved by the local ethics committee (No. EA1/270/16) and conducted in accordance with the Declaration of Helsinki.

Biosample collection

Systemic blood samples (SYS) were obtained during primary percutaneous coronary intervention (PCI) by aspiration of 30 ml blood from the arterial sheath, while local blood samples (LOC) were collected directly from the ACS–causing culprit lesion (LOC) by a the Export Advance™ aspiration catheter system (Medtronic, Minneapolis, MN, USA) (see Supplementary data online, *Material S2*). All experiments were performed in a blinded manner without revealing the underlying ACS–causing pathology to the operator.

Flow cytometry characterization of neutrophil and monocyte receptor repertoire

LOC and SYS whole EDTA–anticoagulated blood samples (100 μl) were stained with a cocktail of fluorochrome-labeled antibodies for a carefully pre-selected set of surface markers expressed by neutrophils and monocytes (see Supplementary data online, *Material S3A*), followed by a 1:10 dilution/fixation in 0.5% phosphate-buffered paraformaldehyde solution (final volume 1000 μl). Samples were acquired 16–24 h afterwards on an Attune NxT Acoustic Focusing Flow Cytometer (Thermo Fisher Scientific, USA), and data were analyzed by the Kaluza v1.5 software (Beckman Coulter Inc., USA) (see Supplementary data online, *Material S3B*, for the gating strategy). The receptor expression density per cell is described by the median fluorescence intensity of each marker. Due to the fact that neutrophils are the main, but not only immune cell population activated immediately after myocardial infarction,[19] we also analyzed the distribution and TLR2 expression of the three main monocyte subtypes: classical (defined as $CD14^{++}$ $CD16^{-}$), intermediate (defined as $CD14^{++}$ $CD16^{+}$), and alternative monocytes (defined as $CD14^{+}$ $CD16^{+}$) using flow cytometry.

Polymorphonuclear granulocyte isolation

Polymorphonuclear granulocytes (PMNs) were isolated from both blood samples (LOC and SYS) using Polymorphprep density separation medium (Alere Technologies AS, Oslo, Norway) according to the manufacturer's instructions.

Matrix metalloproteinase activity in supernatants and plasma samples from isolated PMNs

Isolated PMNs were either activated by a human recombinant TLR2/1 agonist (Pam3CSK4) or pre-treated with a selective inhibitory anti-TLR2 antibody. Fluorescence gelatine zymography was performed according to the manufacturer's instructions (Invitrogen, Fisher Scientific, Göteborg, Sweden) to quantify gelatinase activity of the pre-treated PMNs in a time course. Furthermore, using the same technique the gelatinolytic activity in local and systemic citrate plasma samples was assessed, too.

Gelatine gel zymography of the above described supernatants was used for size discrimination between pro-matrix metalloproteinase (pro-MMP2)/MMP2 (80/72 kDa), pro-MMP9/MMP9 (92/84 kDa), and MMP9/neutrophil gelatinase–associated lipocalin (NGAL) complex (125 kDa) and performed as previously described by Toth et al.[20]

Immuno-enzymatic assay for detection of MMP9, NGAL, and hyaluronic acid plasma concentration

The concentrations of MMP9, NGAL, and hyaluronic acid (HA) in human plasma samples were assessed by commercially available ELISA kits (MMP 9 Human ELISA, Thermo Fischer, USA; NGAL ELISA Kit from Bioporto, Hamburg, and HA Test Kit, Corgenix, Broomfield, CO, USA, respectively). All tests were performed according to the manufacturer's instructions.

Assessment of endothelial cell death and neutrophil survival in co-culture

1×10^6 PMNs, isolated and pre-treated as previously described, were co-cultured with 1×10^5 human aortic endothelial cells (HAECs) for 24 h in a humidified CO_2 incubator (5% CO_2, 37°C). HAECs without the addition of PMNs served as intra-experimental control. After the indicated exposure time, all cells were harvested by trypsinization and labelled with a cocktail of fluorochrome labeled antibodies, following measurement on an Attune Nxt Acoustic Focusing Flow Cytometer (Thermo Fisher Scientific, USA) and evaluation using Kaluza v1.5 (Beckman Coulter Inc., USA) analysis software. The neutrophil survival upon TLR2 activation was assessed directly by AnnexinV/Sytox Orange staining and indirectly by shedding of CD16.[21] For the gating strategy, please refer to Supplementary data online, *Material S4*.

Effect of disturbed flow and recombinant MMP9 on endothelial detachment

HAECs were grown to 80% confluence on 1% gelatine pre-coated double-y-shaped microchannel slides (Ibidi, Gräfelfing, Germany) under laminar flow conditions (12 dyn/cm^2 unidirectional flow). HAECs were either pre-treated with 500 ng/mL human recombinant MMP9 (Enzo Lifesciences, New York, USA) or control growth factor–deprived EBM medium. Endothelial cell detachment under different flow conditions: 'laminar' defined as unidirectional flow with 12 dyn/cm^2 or 'oscillatory' defined as bidirectional flow with 12 dyn/cm^2 was evaluated after 24 h using immunofluorescence stating for phalloidin for F-zctin and Hoechst for cell nuclei. Images showing the % detachment area were taken on a BZ-9000 inverted fluorescence phase contrast microscope (Keyence, USA) in 10× magnification and evaluated using ImageJ software version 1.48 (NIH/University of Wisconsin, USA).

Confocal microscopy immunofluorescence of intracoronary thrombus aspirates

Aspirated thrombus specimens from IFC–ACS and RFC–ACS patients ($n = 20$) were fixed in 4% paraformaldehyde solution, dehydrated in 30% sucrose solution, and embedded in OCT medium for long-term preservation at −80°C.

Assessment of HYAL2 expression in pre-flowed endothelial cell monolayers

Using reverse transcription polymerase chain reaction (RT-PCR), we assessed the gene expression of hyaluronidase 2 (HYAL2) in pre-flowed endothelial cell monolayers as described above. The relative protein expression of HYAL2 (Abcam, USA) to GAPDH (Cell Signaling, The Netherlands) was validated by western blot analysis.

Statistical analysis

Statistical analysis was based on a matched case–control study design. Distributions of variables were reported by standard descriptive statistics as described in the figure legends. Two group comparisons of continuously distributed variables were performed with Wilcoxon matched-pairs signed rank tests and categorical variables by Mc Nemar chi^2 test due to the case–control study design.[22,23] Data with multiple readings within a patient were analyzed by a repeated measures analysis of variance including a factor (group, e.g. plaque phenotype). The overall effect of group, time, and interaction group × time was reported. Multiple post-hoc comparisons were performed in order to test for group differences (e.g. pathology) at each time point with a Bonferroni's correction for multiple comparisons in post-hoc tests. A two-sided $P < 0.05$ was considered to be statistically significant.

In addition, we reported the effect sizes Cohen's *d* (standardized mean difference [SMD])[24] for pairwise comparisons with rules of thumb to evaluate the magnitude of the effect size *d* reported in the figure legends.[25] For ANOVA with repeated measures, we calculated the partial η^2 as an appropriate effect measure with a rule of thumb in the figure legends.[25] Partial η^2 depicts the extent to which the total variance of the outcome (e.g. MMP9 activity) is explained by the covariates (e.g. time and pathology). Statistical analysis was performed with GraphPad Prism Software (La Jolla, CA) and SAS 9.3.

For detailed description of the methods, please refer to Supplementary data online, *Material S5*.

Results

Patients clinical characteristics

The baseline characteristics of the groups were similar, except for the expected higher proportion of dyslipidemia with higher total and LDL cholesterol (*Table 1*) in patients with RFC–ACS, which indeed is the pathophysiological hallmark of a RFC.[8,26] We observed a higher preclinical use of statins in RFC–ACS vs. IFC–ACS (*Table 1*). Furthermore, the matched cohort was considered representative for the main study cohort of the OPTICO–ACS trial (see Supplementary data online, *Material S6*) and well balanced as shown by the SMDs of the continuous baseline characteristics (*Table 2*).

Differences in culprit plaque morphology assessed by optical coherence tomography

In line with the higher proportion of dyslipidemia and culprit features presented recently for the entire OPTICO–ACS study cohort[8] as well as other studies,[27] RFC–ACS–causing culprit plaques were predominantly thin-cap fibroatheromas and were characterized by larger maximum lipid arcs when compared with IFC–ACS culprit lesions (see Supplementary data online, *Material S7*).

Upregulation of TLR2 on neutrophils in IFC–ACS

Absolute neutrophil cell counts and the relative distribution as a ratio of LOC vs. SYS neutrophils were not different between patients with IFC–ACS and RFC–ACS (*Figure 1A*, Supplementary data online, *Material S8*). However, higher expression levels of TLR2 were detected on neutrophils from IFC–ACS patients compared with RFC–ACS patients (*Figure 1B*). The expression levels of the other neutrophil receptors from our pre-defined panel between IFC–ACS and RFC–ACS were similar (see Supplementary data online, *Material S9*), as were the distribution of the monocyte subpopulations and their TLR2 expression between both disease groups (see Supplementary data online, *Material S10* and *S11*). Consequently, in subsequent experiments, we focused on the effect of an *in vitro* TLR2 stimulation of the neutrophils.

Increased local and systemic MMP9 concentration in IFC–ACS vs. RFC–ACS

Another surrogate marker for higher neutrophil-driven inflammatory activity in IFC–ACS was the higher local and systemic MMP9

Table 1 Clinical baseline characteristics of the study cohort. For comparison between categorical parameters, a McNemar test was used; for comparison between continuously distributed parameters, the Wilcoxon matched-pairs signed rank test was used. Values are expressed as a median with interquartile range (IQR); $n = 32$ per group

	RFC–ACS ($n = 32$)	IFC–ACS ($n = 32$)	*P* value
Patient characteristics			
Age (years)	62.0 ± 16.75	61.0 ± 16.5	0.793
Male (*n*;%)	26 (81)	26 (81)	0.999
Family history for CAD (*n*;%)	14 (44)	14 (44)	0.999
Active smoking (*n*;%)	13 (40)	17 (53)	0.459
Diabetes mellitus type 2 (*n*;%)	7 (22)	7 (22)	0.999
Arterial hypertension (*n*;%)	29 (91)	26 (81)	0.214
Dyslipidemia[a] (*n*;%)	30 (94)	22 (68)	**0.002**
BMI (kg/m^2)	25.5 ± 6.1	25.6 ± 3.9	0.652
Previous history of PCI (*n*;%)	6 (19)	1 (3)	0.071
Laboratory data			
Total cholesterol (mg/l)	204.0 ± 61.0	179.0 ± 50.2	**0.040**
LDL cholesterol (mg/l)	129.0 ± 53.0	113.0 ± 44.5	**0.026**
HDL cholesterol (mg/l)	40.0 ± 14.0	50.0 ± 20.0	0.417
Serum creatinine (mg/l)	0.94 ± 0.2	0.97 ± 0.2	0.256
Hemoglobin (g/dl)	14.7 ± 1.8	14.8 ± 1.6	0.681
Leukocytes (per nl)	10.5 ± 4.3	11.0 ± 6.0	0.367
hsCRP (mg/l)	2.1 ± 5.4	2.0 ± 3.2	0.721
ACS characteristics			
Presentation as STE–ACS (*n*;%)	20 (63)	18 (50)	0.298
CK peak (U/l)	902.0 ± 720	569.0 ± 1.063	0.267
LVEF at discharge (%)	59.0 ± 11	55.0 ± 12.5	0.382
Concomitant medication (*n*; %)			
PCSK9 inhibitor	0 (0)	0 (0)	0.241
Ezetimibe	0 (0)	1 (3.1)	0.191
Statin	3 (9.4)	1 (3.1)	**0.010**

RFC–ACS, ruptured fibrous cap—acute coronary syndrome; IFC–ACS, intact fibrous cap acute coronary syndrome; SD, standard deviation; *n*, number; BMI, body mass index; LVEF, left ventricular ejection fraction; hsCRP, high-sensitivity C-reactive protein; CK, creatinine kinase; LDL, low-density lipoprotein; HDL, high-density lipoprotein; STE–ACS, ST-elevation myocardial infarction; PCI, percutaneous coronary intervention.

[a]Defined as TC ≥ 220 mg/dl, triglycerides ≥ 150 mg/dl, LDL-C ≥ 140 mg/dl, HDL-C ≤ 40 mg/dl or taking medication for dyslipidemia. Bold values represent statistically significant results with a p value < 0.05.

	RFC-ACS ($n = 32$)	IFC–ACS ($n = 32$)	*P* value
Culprit segment TIMI flow < 1 (*n*; %)	11 (34%)	8 (25%)	0.219
Culprit vessel (*n*; %)			
LM	0 (0)	1 (3)	0.241
LAD	15 (47)	16 (50)	
LCX	4 (13)	6 (19)	
RCA	13 (41)	9 (28)	
Involved culprit segment (*n*; %)			
Proximal	8 (25)	18 (56)	0.06

Continued

Table 1 ***Continued***

	RFC-ACS ($n = 32$)	IFC–ACS ($n = 32$)	*P* value
Medial	23 (72)	12 (38)	
Distal	1 (3)	2 (6)	
Number of diseased vessels (*n*; %)			
1	16 (50)	22 (69)	0.284
2	9 (28)	6 (19)	
3	7 (22)	4 (13)	
PCI characteristics			
Total stented length (mm)	26.0 ± 30.6	23.0 ± 11.5	0.362
Largest stent diameter (mm)	3.5 ± 0.50	3.4 ± 1.0	0.992

RFC–ACS, ruptured fibrous cap—acute coronary syndrome; IFC–ACS, intact fibrous cap acute coronary syndrome; SD, standard deviation; TIMI, thrombolysis in myocardial infarction; LM, left main; LAD, left anterior descending artery; LCX, left circumflex artery; RCA, right coronary artery.

Table 2 Standardized mean differences (SMDs, *d*) reported for continuous baseline characteristics show well-balanced matched populations; effect size *d* (absolute values of *d*: small effect $d < 0.2$, medium effect *d* between 0.2 and 0.8, large effect $d > 0.8$). Values are expressed as a median with interquartile range (IQR); $n = 32$ per group

	RFC–ACS	IFC–ACS	*d*
PCI characteristics			
Total stented length (mm)	26.0 ± 30.6	23.0 ± 11.5	0.08
Largest stent diameter (mm)	3.5 ± 0.50	3.4 ± 1.0	0.05
Patient characteristics			
Age (years)	62.0 ± 16.75	61.0 ± 16.5	0.04
BMI (kg/m^2)	25.5 ± 6.1	25.6 ± 3.9	0.08
Laboratory data			
Total cholesterol (mg/l)	204.0 ± 61.0	179.0 ± 50.2	0.49
LDL cholesterol (mg/l)	129.0 ± 53.0	113.0 ± 44.5	0.56
HDL cholesterol (mg/l)	40.0 ± 14.0	50.0 ± 20.0	0.23
Serum creatinine (mg/l)	0.94 ± 0.2	0.97 ± 0.2	0.17
Hemoglobin (g/dl)	14.7 ± 1.8	14.8 ± 1.6	0.09
Leukocytes (per nl)	10.5 ± 4.3	11.0 ± 6.0	0.16
hsCRP (mg/l)	2.1 ± 5.4	2.0 ± 3.2	0.19
ACS characteristics			
CK peak (U/l)	902.0 ± 720	569.0 ± 1.063	0.13

concentration in the plasma samples (*Figure 2A* and *B*), as neutrophils represent not the only, but the largest immediate source of MMP9 after a myocardial infarction.[28,29] Furthermore, local plasma samples from IFC–ACS patients showed higher gelatinolytic activity in comparison to RFC–ACS patients (*Figure 2C*). This effect was not observed in systemic samples (*Figure 2D*).

TLR2 activation specifically enhances release and activation of MMP9 from local IFC–ACS neutrophils

Upon TLR2 activation with Pam3CSK4, LOC IFC–ACS–derived neutrophils increased their gelatinolytic activity as compared with lesion-site RFC–ACS neutrophils (*Figure 3A*) and SYS IFC–ACS neutrophils (*Figure 3B*). This effect was observed neither in SYS neutrophils (*Figure 3C*) nor in RFC–ACS neutrophils in general (*Figure 3D*). Exemplary gelatine zymography supported MMP9 to be the predominant gelatinase in the supernatants of the stimulated neutrophils (*Figure 3E*). Furthermore, the local plasma samples from IFC–ACS patients showed an increased concentration of NGAL (*Figure 3F*), which prevents MMP9 inactivation.[30]

Upon TLR2 blockade by an anti-TLR2 antibody, MMP9 activity was not enhanced by Pam3CSK4 stimulation anymore, underlining the specific relation between the TLR2 activation and release of active MMP9 by neutrophils at the culprit lesion site of patients with IFC–ACS (*Figure 4A*). This effect was not observed in RFC–ACS–derived neutrophils in general and SYS IFC–ACS–derived neutrophils (*Figure 4B*, Supplementary data online, *Material S12*).

Aggravated endothelial cell detachment by MMP9 and oscillatory flow

Turbulent flow conditions aggravated endothelial cell detachment exclusively in combination with MMP9 (*Figure 5*).

TLR2 activation prevents neutrophil apoptosis in local IFC–ACS–derived neutrophils

High CD16b expression as an indirect marker of neutrophil survival[21,31,32] was maintained in LOC IFC–ACS–derived neutrophils upon TLR2 activation by Pam3CSK4 (*Figure 6A*). Moreover, in SYS IFC–ACS and RFC–ACS neutrophils in general (*Figure 6A* and *B*), TLR2 activation did not prevent neutrophil apoptosis. This data was supported by a flow cytometry assessment of neutrophil survival, where we observed a decrease in the apoptotic rate of overall and CD16^{lo} IFC–ACS–derived

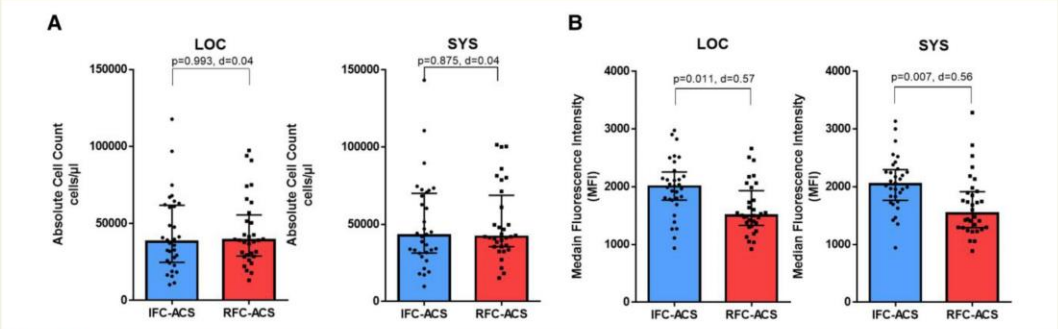

Figure 1 Flow cytometry analysis of neutrophil surface receptors shows equal neutrophil cell count in IFC–ACS vs. RFC–ACS (*A*), but higher TLR2 expression on local and systemic neutrophils from IFC–ACS patients vs. RFC–ACS patients (*B*). Wilcoxon matched-pairs signed rank test; effect size *d* (absolute values of *d*: small effect $d < 0.2$, medium effect *d* between 0.2 and 0.8, large effect $d > 0.8$); data are shown as median with interquartile range (IQR); $n = 32$ per each group. MFI, median fluorescence intensity; RFC–ACS, acute coronary syndrome with ruptured fibrous cap; IFC–ACS, acute coronary syndrome with intact fibrous cap; LOC, local; SYS, systemic; *d*, Cohen's.

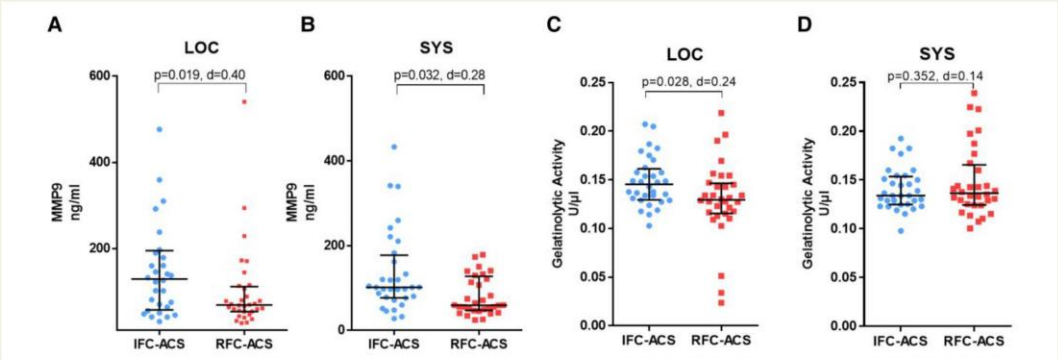

Figure 2 MMP9 concentration in local (*A*) and systemic (*B*) plasma samples from matched patients with IFC–ACS and RFC–ACS, measured in ng/mL; gelatinolytic activity in local (*C*) and systemic (*D*) plasma samples from matched IFC–ACS and RFC–ACS patients, measured in U/µl. Wilcoxon matched-pairs signed rank test; effect size *d* (absolute values of *d*: small effect $d < 0.2$, medium effect *d* between 0.2 and 0.8, large effect $d > 0.8$); data are presented as median with interquartile range (IQR); $n = 32$ per group. MMP9, matrix metalloproteinase 9; LOC, local; SYS, systemic; d = Cohen's.

neutrophils upon TLR2 activation in comparison to RFC–ACS neutrophils (see Supplementary data online, *Material S13* and *S14*).

Aggravated endothelial cell death in co-culture with local IFC–ACS neutrophils

Furthermore, LOC IFC–ACS, but not RFC–ACS–derived neutrophils, enhanced the rate of endothelial cell death, independently of TLR2 (*Figure 7*). Neutrophils from the systemic withdrawal site of IFC–ACS as compared with RFC–ACS did not affect endothelial cell survival (*Figure 8*).

Elevated local hyaluronic acid concentration in IFC–ACS as endogenous activator of TLR2

In line with the observed selective TLR2 activation of LOC neutrophils from IFC–ACS patients, the immuno-enzymatic assays showed that the plasma concentration of HA, a well-known endogenous TLR2 ligand,[33] was similar at SYS levels between patients presenting with IFC–ACS and RFC–ACS, while its LOC plasma levels were slightly higher in the IFC–ACS group (*Figure 9*).

Thrombus aspirates from IFC–ACS patients display high HYAL2 levels and a characteristic HYAL2 distribution

Confocal imaging of thrombus aspirates revealed that specimen collected from patients with IFC–ACS show higher HYAL2 expression than that from RFC–ACS patients, observed mainly at the outer surface of the thrombus, which was exposed to the blood stream (*Figure 10*). Exemplary thrombus sections for IFC–ACS and RFC–ACS are shown in Supplementary data online, *Material S15*. Furthermore, a trend towards higher local presence of neutrophils

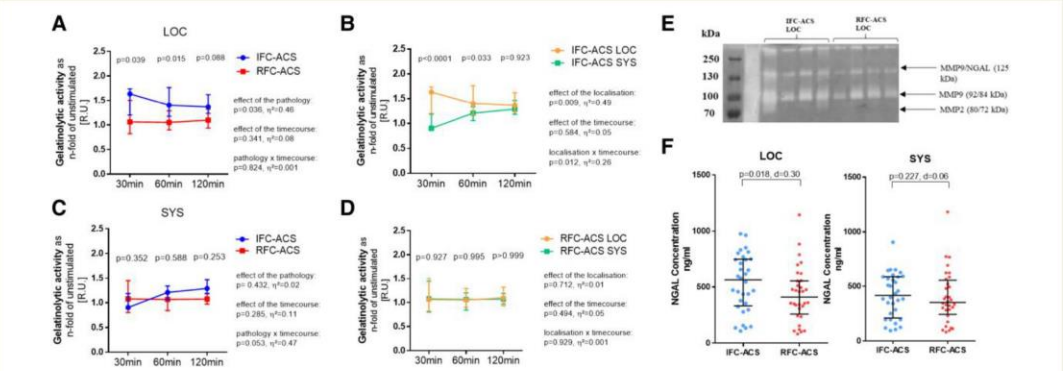

Figure 3 Higher gelatinolytic activity independent of the time course in local IFC–ACS ($n = 8$) vs. RFC–ACS TLR2 pre-treated neutrophils ($n = 8$) (*A*) and in local vs. systemic IFC–ACS neutrophils (*B*). TLR2 activation has no significant effect on the gelatinolytic activity in systemic IFC–ACS vs. RFC–ACS neutrophils (*C*) and in local vs. systemic RFC–ACS neutrophils (*D*); gelatinolytic activity measured in RU and expressed as *n*-fold of the unstimulated control group; representative graphic of gelatinolytic activity of supernatants of TLR2 pre-stimulated neutrophils assessed by gel zymography showing the pre-dominant MMP9 (*E*); local plasma samples from IFC–ACS patients show higher NGAL concentration than RFC–ACS patients as estimated by a Wilcoxon matched-pairs signed rank test, $n = 32$ per group (*F*); for all of the other comparisons, a repeated measures ANOVA with Bonferroni's multiple comparisons test has been used; data are shown as median ± interquartile range (IQR); effect size η^2 after repeated measures ANOVA (small effect $\eta^2 < 0.01$, medium effect η^2 between 0.01 and 0.14, large effect $\eta^2 > 0.14$), effect size *d* (absolute values of *d*: small effect $d < 0.2$, medium effect *d* between 0.2 and 0.8, large effect $d > 0.8$). RFC–ACS, acute coronary syndrome with ruptured fibrous cap; IFC–ACS, acute coronary syndrome with intact fibrous cap; RU, relative units; LOC, local; SYS, systemic; NGAL, neutrophil gelatinase-associated lipocalin; *d* = Cohen's.

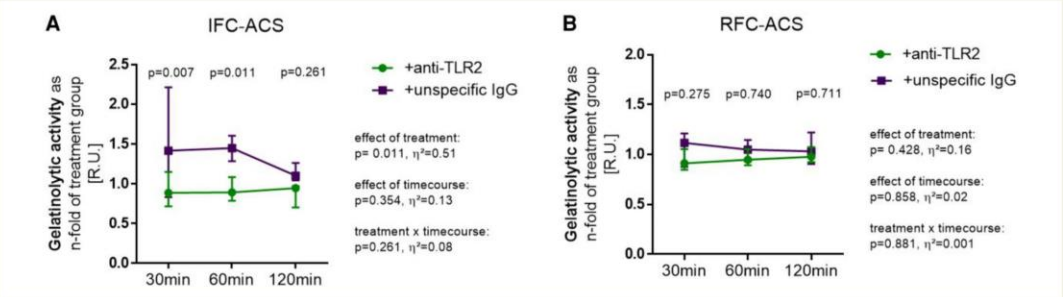

Figure 4 TLR2 inhibition by a monoclonal antibody against TLR2 leads to markedly decreased MMP9 activity in local neutrophils from IFC–ACS (*A*) but not RFC–ACS patients (*B*) measured in RU and expressed as *n*-fold of the TLR2-stimulated group (+Pam3CSK4); $n = 6$ per group; repeated measures ANOVA with Bonferroni's multiple comparisons test; data are shown as median ± interquartile range (IQR); effect size η^2 after repeated measures ANOVA (small effect $\eta^2 < 0.01$, medium effect η^2 between 0.01 and 0.14, large effect $\eta^2 > 0.14$).

in IFC–ACS thrombi was observed by co-staining of neutrophil elastase (NE) and 4′,6-diamidino-2-phenylindole (DAPI) (see Supplementary data online, *Material S16*). Exemplary images of IFC–ACS thrombi implicate co-localization of HYAL2 and neutrophils in the border zones of the thrombi (white arrows in Supplementary data online, *Material S16*).

Endothelial cells do not upregulate HYAL2 under oscillatory shear stress

Under oscillatory flow conditions, endothelial cells interestingly reduce HYAL2 mRNA expression but do not downregulate the protein expression of HYAL2 in comparison to laminar flow conditions (see Supplementary data online, *Material S17*), thus pointing to another cell source of HYAL2 in the context of plaque erosion.

Discussion

In contrast to the well-characterized pathophysiology of RFC–ACS with the main target at the optimization of lipid accumulation, IFC–ACS represents an ACS–causing entity with rising prevalence, but still poorly understood underlying mechanisms, involving genetic/epigenetic pre-disposition, disturbed flow, and particularly distinct inflammatory

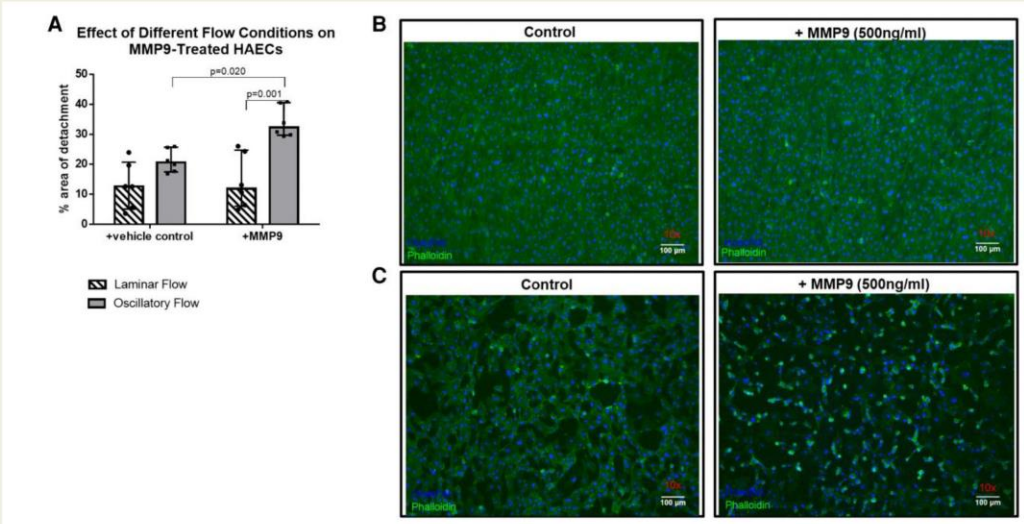

Figure 5 The combination of MMP9 and turbulent (oscillatory) flow leads to increased detachment of HAECs *in vitro* (*A*). Histological sections of HAECs showing normal detachment under laminar flow conditions (*B*) and increased detachment under proatherogenic oscillatory conditions, especially when combined with recombinant MMP9 (*C*); $n = 6$ per group; repeated measures ANOVA with Bonferroni's multiple comparisons test; data are shown as median with interquartile range (IQR).

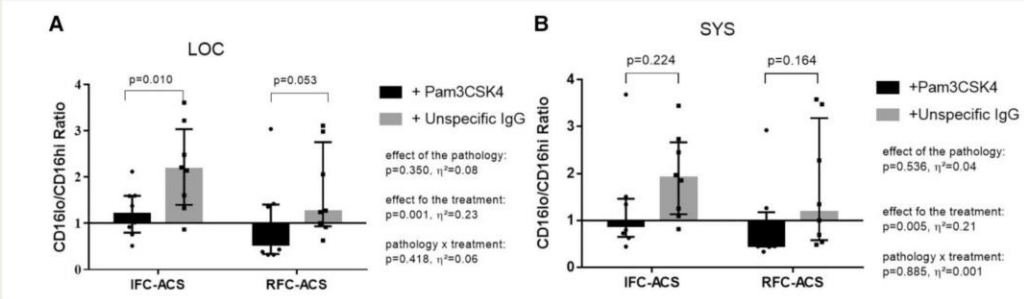

Figure 6 TLR2 activation with Pam3CSK4 increases survival in local IFC–ACS–derived neutrophils (*A*), but neither in systemic IFC–ACS neutrophils (*B*), nor in RFC–ACS–derived neutrophils in general (*A* for local, *B* for systemic); data are expressed as a ratio of CD16lo vs. CD16hi neutrophils. Repeated measures ANOVA with Bonferroni's multiple comparisons test; data are presented as a median with interquartile range (IQR); $n = 8$ per group; effect size η^2 after repeated measures ANOVA (small effect $\eta^2 < 0.01$, medium effect η^2 between 0.01 and 0.14, large effect $\eta^2 > 0.14$). Pam3CSK4, Toll-like receptor 2 ligand; IFC–ACS, acute coronary syndrome with intact fibrous cap; RFC–ACS, acute coronary syndrome with ruptured fibrous cap.

activation patterns.[8,10,34] With the development of intracoronary imaging, it has become feasible to characterize the morphology of the culprit lesion *in vivo* and thereby to distinguish between different ACS–causing pathologies in real time and not only post-mortem.[35] This allows for development of precise-targeted treatment approaches for different ACS patient populations, which itself requires better understanding of the underlying pathophysiological mechanisms.

Since neutrophils have been proposed to be a key initiator of the progression and destabilization of the ACS–causing culprit plaques,[10] our study focuses on the differences in the neutrophil activation between the two main ACS–causing pathophysiologies (IFC- and RFC–ACS). The study implicates an increased TLR2-dependent neutrophil activation and MMP9 release, presumably triggered by elevated HA and enhanced by disturbed flow conditions in patients with IFC–ACS (*Structured Graphical Abstract*). The provided inpatient functional data sharpen our mechanistic understanding of IFC–ACS and propose future prevention and therapeutic targets for this patient population.

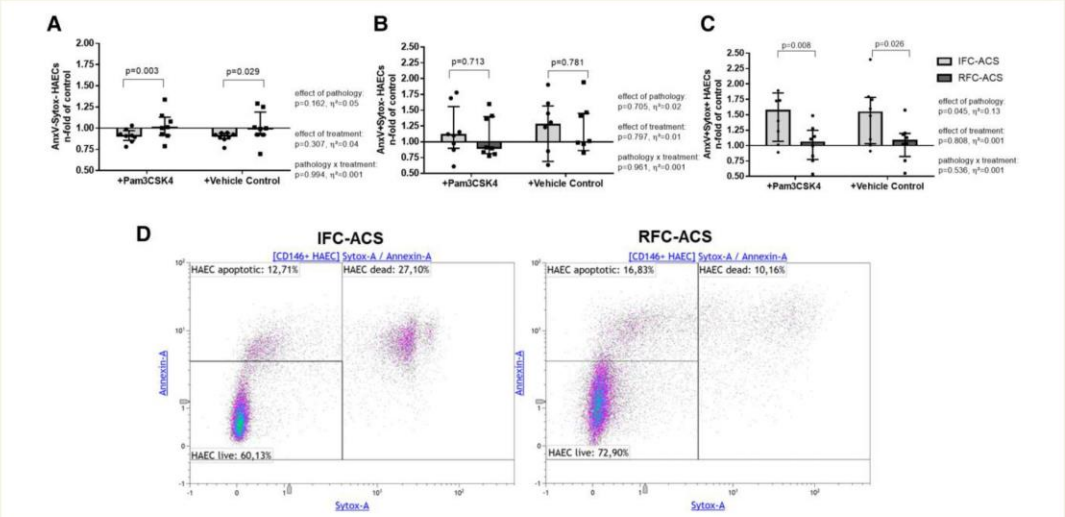

Figure 7 Increased rate of dead AnxV+Sytox + endothelial cells (*C*) in co-culture with either Pam3CSK4 pre-treated or non-treated (vehicle control) local neutrophils from IFC–ACS patients, but not RFC–ACS patients; no effect on live AnxV-Sytox- HAECs (*A*) and apoptotic AnxV + Sytox- HAECs (*B*); representative images of the applied gating startegy (D); repeated measures ANOVA with Bonferroni's multiple comparisons test; data are presented as a median with interquartile range (IQR); $n = 8$ per group; effect size η^2 after repeated measures ANOVA (small effect $\eta^2 < 0.01$, medium effect η^2 between 0.01 and 0.14, large effect $\eta^2 > 0.14$). Pam3CSK4, Toll-like receptor 2 ligand; AnxV, Annexin V; HAECs, human aortic endothelial cells.

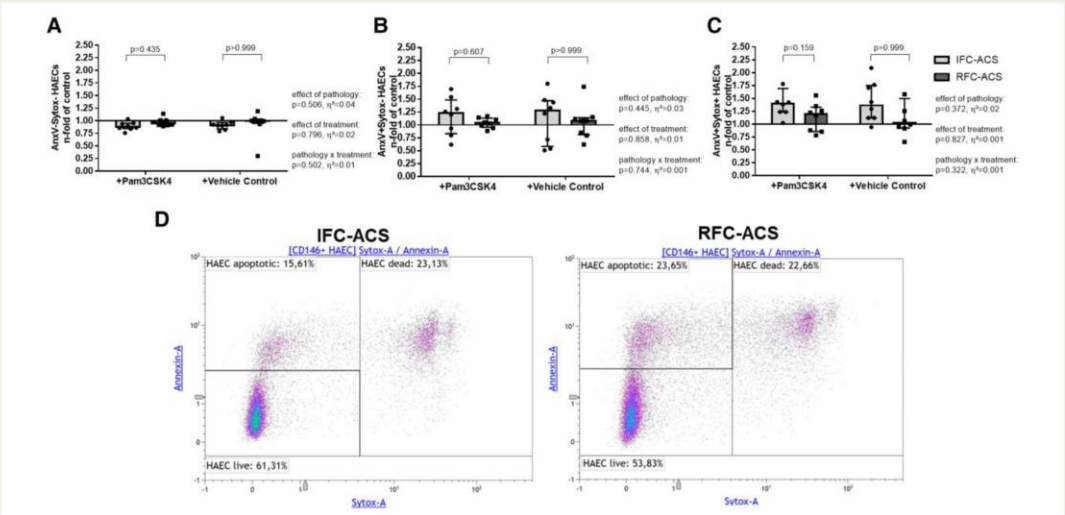

Figure 8 Constant rate of live (AnxV- Sytox-, A), apoptotic (AnxV+ Sytox-, B) and dead (AnxV + Sytox +, C) endothelial cells in co-culture with either Pam3CSK4 pre-treated or non-treated (vehicle control) systemic neutrophils from IFC–ACS and RFC–ACS patients; representative images of the applied gating strategy (D); repeated measures ANOVA with Bonferroni's multiple comparisons test; data are presented as a median with interquartile range (IQR); $n = 8$ per group; effect size η^2 after repeated measures ANOVA (small effect $\eta^2 < 0.01$, medium effect η^2 between 0.01 and 0.14, large effect $\eta^2 > 0.14$). Pam3CSK4, Toll-like receptor 2 ligand; AnxV, annexin V; HAECs, human aortic endothelial cells; IFC–ACS, acute coronary syndrome with intact fibrous cap; RFC–ACS, acute coronary syndrome with ruptured fibrous cap.

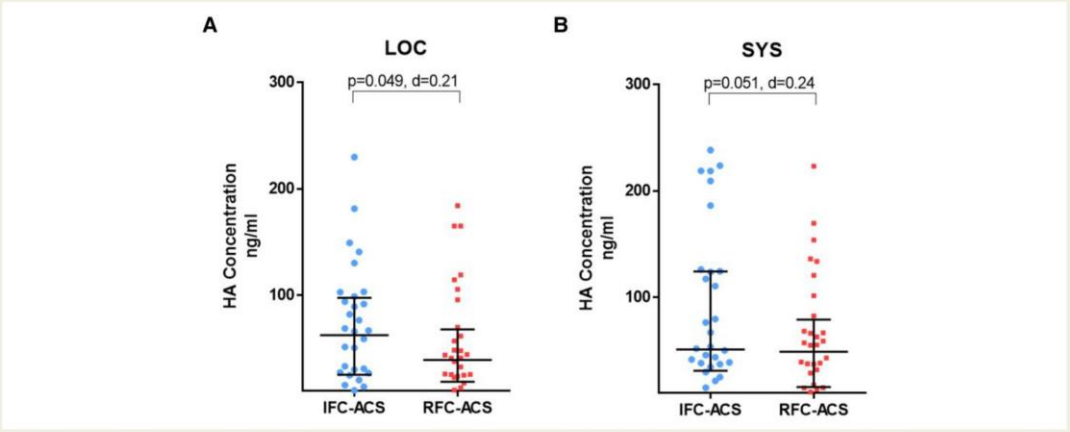

Figure 9 Scatter plots with bars showing HA concentrations (ng/mL) in local (*A*) and systemic (*B*) plasma samples from matched IFC–ACS vs. RFC–ACS patients. Wilcoxon matched-pairs signed rank test; effect size *d* (absolute values of *d*: small effect $d < 0.2$, medium effect *d* between 0.2 and 0.8, large effect $d > 0.8$); data are presented as median with interquartile range (IQR); $n = 32$ per group. HA, hyaluronan; LOC, local; SYS, systemic; *d* = Cohen's.

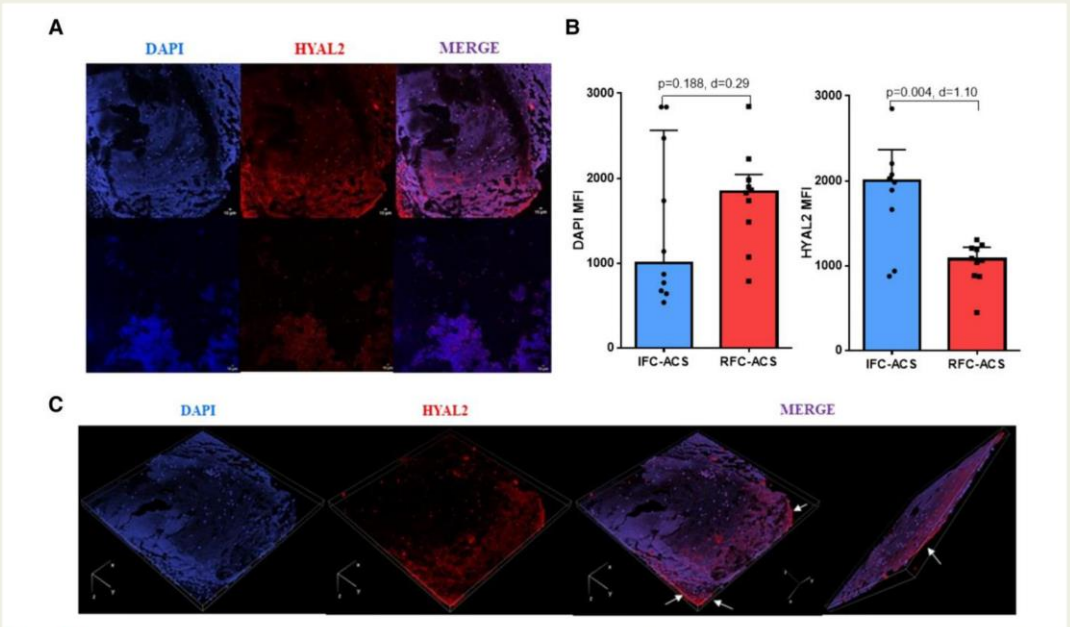

Figure 10 (*A*) Immunofluorescence analyses assessed by confocal microscopy showing DAPI and HYAL2 levels. Samples were stained with DAPI and HYAL2 antibody . Merge of the two labels is showed as composite image (co-expression of DAPI and HYAL2). Bars represent 10 μm. Images were taken at 20× magnification and at resolutions of 512 × 512. (*B*) Scatter plot with bars showing the DAPI and HYAL2 expressed as MFI (*C*) 3D representative projection of a sample of a coronary thrombus aspirated from a patient with plaque erosion created through a multiple stack series acquisition (dimension order: XYCZT). White arrows indicate the area of HYAL2 intense immunoreactivity; Wilcoxon matched-pairs signed rank test; effect size *d* (absolute values of *d*: small effect $d < 0.2$, medium effect *d* between 0.2 and 0.8, large effect $d > 0.8$); data are presented as median with interquartile range (IQR). DAPI, 4′,6-diamidino-2-phenylindole; HYAL2, hyaluronidase-2; mm, micrometer; MFI, mean fluorescence intensity; *d* = Cohen's.

Neutrophil activation in IFC–ACS: a question of functionality and not cell count

Neutrophil infiltration is both observed in atherosclerotic culprit lesions from RFC–ACS and IFC–ACS patients,[36] but their exact functional properties in the context of these pathologies are still incompletely understood. Therefore, this study aimed to better characterize the activation patterns of human neutrophils from patients with IFC–ACS as compared with RFC–ACS.

While previous studies show mainly quantitative alterations, i.e. of neutrophil count in ACS,[37] the current study highlights a different functionality with an increased TLR2 expression of the neutrophils in IFC–ACS, despite similar neutrophil abundance. Previous murine and *in vitro* data converge on a 'two-hits' model of plaque erosion: injured endothelium at localizations with high shear stress expresses higher levels of TLR2 and thereby acts as a trigger for the second hit: the neutrophil attraction and activation, which aggravates the endothelial cell detachment and thereby leads to plaque erosion.[11] The current study advances this concept by providing complementary first-in-human data on IFC–ACS–derived neutrophils in a more disease-centered approach, showing specific TLR2-dependent mechanisms of neutrophil activation and MMP9 release and thereby suggesting potential therapeutic targets for this patient population.

TLR2-dependent neutrophil activation in IFC–ACS

The involvement of TLRs in sterile inflammatory diseases such as autoimmune diseases and atherosclerosis was postulated in the beginning of the 21st century by showing interactions with endogenous molecules like HA and other damage-associated molecular patterns.[38] Intriguingly, histological evidence shows that especially IFC–ACS lesions contain high amounts of HA,[33,39] suggesting that local exposure of HA and in particular low-molecular-weight hyaluronic acid (LMW-HA) may trigger innate immune response in plaque erosion via TLR2.[33,39–41] LMW-HA is capable of inducing quick recruitment and activation of classical innate immune cells such as monocytes[42] and neutrophils.[33] In correspondence, we observed not only higher expression of TLR2 exclusively on local neutrophils and not monocytes from IFC–ACS patients but also higher abundance of HYAL2, the key enzyme responsible for the HA catabolism and release into the bloodstream,[43] in the thrombus material from patients with plaque erosion. This finding may account for the observed increased concentration of HA in the local plasma samples of the IFC–ACS patients. In this context, our study provides a plausible association between the higher HYAL2 expression with correspondingly higher HA local concentrations and the subsequent activation of the TLR2 on neutrophils as one of the pathophysiological mechanisms in IFC–ACS.

In order to study the functional impact of the TLR2 activation in neutrophils, we mimic the endogenous TLR2 activation of isolated neutrophils from IFC–ACS and RFC–ACS patients by stimulating them *ex vivo* and studying their differential inflammatory response. Nevertheless, for this purpose, we used an agonist of the TLR2/TLR1 heterodimer: Pam3CSK4 and not HA in order to study the TLR2-specific response of neutrophils and not the general HA-driven activation of also other HA-binding receptors. As demonstrated by the current study, IFC–ACS–derived neutrophils do not only express higher amounts of TLR2 compared with RFC–ACS neutrophils, but the TLR2 pathway appears to be generally more susceptible to activation as shown by an increased release of MMP9 at the local site of IFC–ACS and not systemically, suggesting a disease-specific pattern. In this context, we consider the increased expression of HYAL2 in the coronary thrombi and thereby the increased local concentration of cleaved HA as one of the main amplifier of the TLR2-mediated neutrophil activation in IFC–ACS, determining their reaction specificity at the lesional site and not elsewhere in the artery system. The reaction specificity appears also to be determined by the fact that high shear stress, which is normally ubiquitous in the artery system, does not increase the HYAL2 expression in endothelial cells, supporting previous studies showing that lesional monocytes, but not the endothelium itself, seem to be the main source of HYAL2.[39] In this context, our immunofluorescence analysis shows a tendency towards a co-localization of HYAL2 and neutrophils in IFC–ACS thrombi, thereby proposing neutrophils as possible HYAL2 sources themselves and thereby also supporting the hypothesis of HYAL2 originating rather from immune cells than from endothelial cells in IFC–ACS.

TLR2-dependent increase in MMP9 secretion by IFC–ACS–derived neutrophils

Obviously, more factors are simultaneously required for the TLR2-dependent neutrophil activation: not only the higher TLR2 expression by the LOC IFC–ACS–derived neutrophils but also the distinct local environment of the IFC–ACS causing culprit lesion, rich in endogenous TLR2 ligands like LMW-HA[39] and characterized by a distinct inflammatory signature as depicted in the Structured Graphical Abstract.[8]

Upon TLR2 stimulation of LOC IFC–ACS neutrophils, we observe an increase in the secretion of active MMP9. This effect was not seen in SYS IFC–ACS, nor in RFC–ACS neutrophils, and was shown to be reversible under TLR2 blockade, supporting a specific TLR2-dependent neutrophil activation pattern at the site of the culprit lesion in plaque erosion. Correspondingly, we observe higher local MMP9 concentrations in plasma samples obtained from the culprit site of IFC–ACS as compared with RFC–ACS, which might originate from LOC neutrophils from IFC–ACS patients, with greater sensitivity towards locally available TLR2 substrates, e.g. HA.[40]

In contrast to the well-established role of MMP9 in plaque rupture and fissure,[44] where increased MMP9 concentration is associated with plaque instability due to collagen breakdown inside the coronary vessel wall,[45,46] little is known about its contribution to the pathology of plaque erosion due to a different localization of action: the blood stream.[47] The different localization of the immune cells and their secretory mediators seems to be of a great importance for the better understanding of the pathology of RFC–ACS and IFC–ACS. RFC–ACS–causing lesions are characterized by more prone infiltration of immune cells into the vessel wall,[48,49] whereby in IFC–ACS, the inflammatory cascade is mainly taking place intraluminal;[8,10] therefore, our study design focuses on the local intraluminal environment at the culprit lesion.

One hypothesis suggests that intraluminal cleavage of non-fibrillar collagen, such as collagen IV, by gelatinases (MMP2 and MMP9)[50] may lead to degradation of the basal membrane to which endothelial cells attach and thereby trigger endothelial cell desquamation as a hallmark of plaque erosion.[10,34] In a proof-of-concept *in vitro* experiment, we demonstrate that recombinant human MMP9 aggravates endothelial cell detachment in a flow chamber mimicking coronary artery bifurcations, which might point to the requirement of both factors, i.e. flow conditions and active MMP9, for the initiation of IFC–ACS. This seems to be in line with our previous observation that the culprit lesion is more frequently located close to bifurcations in IFC than in RFC–ACS.[8]

Furthermore, MMP9 may function as an important positive feedback loop for neutrophil chemotaxis and activation by cleaving pro-interleukin (IL)1β and IL8 into their active forms.[51]

As shown by some studies, one of the major sources of active MMP9 after myocardial infarction is the neutrophils themselves[52] and their ability to quickly release MMP9 from their storage in secondary granulae designates them to be the immediate source of MMP9 after acute myocardial infarction.[28,53] However, the impact of MMP9 on the post-infarct remodeling of the myocardium is controversially discussed due to the two-sided role of MMP9 depending on the timing after myocardial infarction. On the one hand, high MMP9 levels in the early phase are associated with higher neutrophil counts and seem to have detrimental effects on left ventricular remodeling; on the other hand, increased MMP9 concentrations in the late phase of wound healing are associated with preservation of left ventricular function.[54] Therefore, further investigation into the impact of MMP9 on post-infarct remodeling, specifically in the context of IFC–ACS, is needed in order to develop precise therapeutic targets with negligible off-side effects, which however extends beyond the scope of the current hypothesis-generating study.

TLR2-independent neutrophil cytotoxicity in IFC–ACS

Furthermore, our study points toward another possible cellular mechanism of IFC–ACS: direct cytotoxic effects of activated neutrophils on endothelial cells.[10] We have previously postulated T-cell–mediated cytotoxicity as one of the main contributors to endothelial cell death in plaque erosion.[8] However, MMP9 may function as a cross-link between the innate and adaptive immunity by cleaving the functional domain of CD31 on $CD4^+$ T-cells and thereby inducing T-cell dysregulation, as exemplary shown in non-ST-elevation myocardial infarction patients.[55] However, not only T-cell–mediated cytotoxicity but also neutrophil cytotoxicity towards endothelial cells seems to play an important role in IFC–ACS, as it was suggested to be higher than of neutrophils isolated from RFC–ACS patients and was independent of the TLR2 activation, thereby proposing a complementary mechanism of endothelial cell loss in IFC–ACS. This might involve NETosis[56,57] or cytotoxic effects of the neutrophil secretome as previously shown,[58] which have not been the focus of the current study and may represent promising neutrophil activation pathways to be further examined in future studies.

TLR2 activation prolongs neutrophil survival in IFC–ACS

The whole process may be further boosted by a decreased apoptosis rate of local IFC–ACS–derived neutrophils upon TLR2 engagement, which may lead to prolonged neutrophil activation at the culprit site of IFC–ACS as suggested by the current study. The importance of maintaining a healthy neutrophil turnover is shown in infectious diseases such as sepsis, where neutrophil survival, infiltration, and damage of vital organs such as the lungs, kidneys, and heart are aggravated in a TLR2-dependent manner.[59,60]

In this context, the presented study emphasizes the associative involvement of many different local factors in the neutrophil activation at the lesion site of IFC–ACS with TLR2 activation being one of the main drivers of neutrophil MMP9 release and neutrophil survival, which may presumably lead to detachment of endothelial cells, especially under turbulent flow conditions, and thereby thrombus formation at the culprit site of plaque erosion (Structured Graphical Abstract).

Anti-TLR2 treatment in IFC–ACS: translational opportunities

In this context, a protective role of temporary anti-TLR2 treatment seems to be plausible as shown for other diseases like early sepsis.[61] The beneficial effects of anti-TLR2 treatment in rats with transient focal ischemia-induced brain damage through inhibition of neuroinflammation were previously demonstrated by Ziegler *et al.*[62] In the context of cardiovascular inflammation, experimental data suggest that inhibition of the TLR2 pathway either by monoclonal antibodies or in a TLR2 knockout mouse model may reduce cardiac fibrosis by attenuating macrophage-mediated cardiac infiltration and subsequent inflammation.[63] Furthermore, a post-infarct treatment with a humanized anti-Toll-like receptor 2 antibody (OPN-305) seems to reduce the infarct size by 45% and enhance cardiac function in a porcine model of ischemia/reperfusion.[64] Yet, only experimental data on anti-TLR2 treatment exist so far, as some limitations like increased mortality due to infections[61] of this therapeutic approach has come to light.

Another potential therapeutic target could be the modulation of the HYAL2 activity in IFC–ACS patients and thereby reducing the amount of HA which may lead to lower TLR2 activation in neutrophils. Hyaluronidase-triggered anticancer treatment has shown promising results in drug-resistant breast cancer.[65] Furthermore, there is some evidence for the anti-thrombotic potential of an anti-HYAL2 treatment through prevention of platelet–monocyte aggregates in ACS.[42] The effect of a similar therapeutic intervention on the TLR2-dependent activation of the neutrophils specifically in IFC–ACS remains to be studied and may represent a therapeutic approach with limited side effects due to careful timing and pre-selection of the patient population. In this regard, developing a profound understanding of the multiple complex events involved in IFC–ACS (Structured Graphical Abstract) and pre-selecting the target population seem to be one of the crucial steps in the development of a successful immunotherapy in patients with IFC–ACS.[66]

Limitations of the study

As typical for studies of acute clinical events, we lack information about the inflammatory activation status at a 'baseline' time point before the acute coronary event. Therefore, we may only speculate about the inflammatory activation status and the underlying pathophysiological mechanisms before the collection time point. Correspondingly, we can mimic the involvement/connection of some activation factors *ex vivo*, but we are limited by default in complete restoration of the exact timing and sequence of occurrence of different factors as it is happening *in vivo*, which of course allows mainly for associative assumptions of the whole pathophysiological process.

Furthermore, the matching strategy may control for some known covariates of neutrophil activation but still leaves some other possible factors unconsidered. Therefore, residual confounding cannot be ruled out completely, which should be taken into consideration when analyzing the data. Due to the small sample size, multivariable analysis was not performed.

We used Pam3CSK4 as a synthetic TLR2/TLR1 agonist, which does not inform on the activation of TLR2/6 in the current context. Even though the same intracellular pathway is being demonstrated for both heterodimers by previous studies,[67] we may still see some different biological effects due to off-target activation of other pathways depending on the ligand being used,[68] which should be taken into account when analyzing the results.

In the current study, we focused on HA as a known endogenous ligand of TLR2 based on previous knowledge about the HA distinct abundance[4,10,39] and metabolism[39] in plaque erosion, but the use of broad proteomics approaches in order to identify possible new TLR2

endogenous ligands is of future interest to our group. We measured total HA concentration and not specifically LMW-HA as methods available for HA size differentiation have significant constraints and require many purification steps with the removal of plasma proteins, use of filters, etc. and thereby may create artefacts and affect the reliability of the results.[69–71] Nevertheless, in the blood stream in contrast to synovial fluids,[72,73] HA polymers are naturally degraded by hyaluronidase to its LMW counterpart.[72–74]

Conclusion

In conclusion, the current study suggests a multiple-hit hypothesis of plaque erosion with distinct TLR2-dependent neutrophil activation, presumably perpetuated by a higher local expression of HYAL2 and thereby increased local cleavage of HA at the coronary culprit lesion of IFC–ACS, leading to enhanced release of active MMP9 by neutrophils and thereby aggravated detachment of luminal endothelial cells in combination with disturbed flow conditions (Structured Graphical Abstract). These data emphasize not only the importance of the TLR2 pathway in patients with IFC–ACS but also the generally aggravated TLR2-independent neutrophil cytotoxicity towards endothelial cells as a hallmark of plaque erosion. MMP9 might further function as a connection between the innate and adaptive immunity, triggering a complementary T-cell–mediated response in IFC–ACS.[8] Thereby, the current study sharpens our understanding of the complex pathology of IFC–ACS, showing that many different factors seem to be simultaneously involved in the inflammatory cascade of IFC–ACS. Further studies need to address the potential therapeutic value of these findings with focus on a possible specific inflammation-targeted treatment of IFC–ACS in the era of personalized medicine.

Acknowledgements

Thanks are due to S. Knüppel and N. Rösener for the technical assistance.

Supplementary data

Supplementary data are available at *European Heart Journal* online.

Declarations

Disclosure of Interest

Abbott, Amgen, AstraZeneca and Daiichi Sankyo (UL, FC, GL, DL), NovoNordisk, Sanofi, Amarin, Berlin-Chemie, Novartis, Pfizer, CRISPR Therapeutics, Bayer, Boeringer Ingelheim and Cardiac Dimensions (UL), Menarini and Chiesi (FC). American Heart Association, Italian National Health Service and Italian Minister of Education (GL).

Data Availability

The data underlying this article will be shared on reasonable request to the corresponding author.

Funding

German Centre for Cardiovascular Research (DZHK) Partner site Berlin, Berlin Institute of Health (BIH) and Italian National Project Grant PRIN 2017, Protocol 2017WJBKKW_001.

Ethical Approval

The study was approved by the local ethics committee (No. EA1/270/16) and conducted in accordance with the Declaration of Helsinki.

Pre-registered Clinical Trial Number

The pre-registered clinical trial number is NCT03129503.

References

1. Dagenais GR, Leong DP, Rangarajan S, Lanas F, Lopez-Jaramillo P, Gupta R, *et al.* Variations in common diseases, hospital admissions, and deaths in middle-aged adults in 21 countries from five continents (PURE): a prospective cohort study. *Lancet* 2020;**395**:785–794. https://doi.org/10.1016/S0140-6736(19)32007-0
2. Vaduganathan M, Mensah GA, Turco JV, Fuster V, Roth GA. The global burden of cardiovascular diseases and risk a compass for future health. *J Am Coll Cardiol* 2022;**80**:2361–2371. https://doi.org/10.1016/j.jacc.2022.11.005
3. Vinci R, Pedicino D, Bonanni A, d'Aiello A, Pisano E, Ponzo M, *et al.* Monocyte-platelet aggregates triggered by CD31 molecule in non-ST elevation myocardial infarction: clinical implications in plaque rupture. *Front Cardiovasc Med* 2022;**8**:741221. https://doi.org/10.3389/fcvm.2021.741221
4. Virmani R, Burke AP, Farb A, Kolodgie FD. Pathology of the vulnerable plaque. *J Am Coll Cardiol* 2006;**47**:C13–C18. https://doi.org/10.1016/j.jacc.2005.10.065
5. Abdelwahed YS, Nelles G, Frick C, Seppelt C, Meteva D, Stahli BE, *et al.* Coexistence of calcified- and lipid-containing plaque components and their association with incidental rupture points in acute coronary syndrome-causing culprit lesions: results from the prospective OPTICO-ACS study. *Eur Heart J Cardiovasc Imaging* 2022;**23**:1598–1605. https://doi.org/10.1093/ehjci/jeab247
6. Jia HB, Abtahian F, Aguirre AD, Lee S, Chia S, Lowe H, *et al.* In vivo diagnosis of plaque erosion and calcified nodule in patients with acute coronary syndrome by intravascular optical coherence tomography. *J Am Coll Cardiol* 2013;**62**:1748–1758. https://doi.org/10.1016/j.jacc.2013.05.071
7. Montone RA, Vetrugno V, Camilli M, Russo M, Fracassi F, Khan SQ, *et al.* Macrophage infiltrates in coronary plaque erosion and cardiovascular outcome in patients with acute coronary syndrome. *Atherosclerosis* 2020;**311**:158–166. https://doi.org/10.1016/j.atherosclerosis.2020.08.009
8. Leistner DM, Krankel N, Meteva D, Abdelwahed YS, Seppelt C, Stahli BE, *et al.* Differential immunological signature at the culprit site distinguishes acute coronary syndrome with intact from acute coronary syndrome with ruptured fibrous cap: results from the prospective translational OPTICO-ACS study. *Eur Heart J* 2020;**41**:3549–3560. https://doi.org/10.1093/eurheartj/ehaa703
9. Meteva D, Seppelt C, Abdelwahed YS, Leistner DM. Distinct pathological mechanisms distinguish acute coronary syndrome caused by plaque erosion from plaque rupture. *Curr Opin Cardiol* 2021;**36**:793–797. https://doi.org/10.1097/HCO.0000000000000912
10. Libby P, Pasterkamp G, Crea F, Jang IK. Reassessing the mechanisms of acute coronary syndromes the "vulnerable plaque" and superficial erosion. *Circ Res* 2019;**124**:150–160. https://doi.org/10.1161/CIRCRESAHA.118.311098
11. Quillard T, Araujo HA, Franck G, Shvartz E, Sukhova G, Libby P. TLR2 And neutrophils potentiate endothelial stress, apoptosis and detachment: implications for superficial erosion. *Eur Heart J* 2015;**36**:1394–1404. https://doi.org/10.1093/eurheartj/ehv044
12. Damman P, van 't Hof AW, Ten Berg JM, Jukema JW, Appelman Y, Liem AH, *et al.* 2015 ESC guidelines for the management of acute coronary syndromes in patients presenting without persistent ST-segment elevation: comments from the Dutch ACS working group. *Neth Heart J* 2017;**25**:181–185. https://doi.org/10.1007/s12471-016-0939-y
13. Ibanez B, James S, Agewall S, Antunes MJ, Bucciarelli-Ducci C, Bueno H, *et al.* 2017 ESC Guidelines for the management of acute myocardial infarction in patients presenting with ST-segment elevation: the Task Force for the management of acute myocardial infarction in patients presenting with ST-segment elevation of the European Society of Cardiology (ESC). *Eur Heart J* 2018;**39**:119–177. https://doi.org/10.1093/eurheartj/ehx393
14. Bailey KL, Smith LM, Heires AJ, Katafiasz DM, Romberger DJ, LeVan TD. Aging leads to dysfunctional innate immune responses to TLR2 and TLR4 agonists. *Aging Clin Exp Res* 2019;**31**:1185–1193. https://doi.org/10.1007/s40520-018-1064-0
15. van Duin D, Mohanty S, Thomas V, Ginter S, Montgomery RR, Fikrig E, *et al.* Age-associated defect in human TLR-1/2 function. *J Immunol* 2007;**178**:970–975. https://doi.org/10.4049/jimmunol.178.2.970
16. Simmons SR, Tchalla EYI, Bhalla M, Bou Ghanem EN. The age-driven decline in neutrophil function contributes to the reduced efficacy of the pneumococcal conjugate vaccine in old hosts. *Front Cell Infect Microbiol* 2022;**12**:849224. https://doi.org/10.3389/fcimb.2022.849224
17. Alfhili MA, Alsughayyir J, Basudan A, Ghneim HK, Aboul-Soud MAM, Marie M, *et al.* Isolated and combined effect of age and gender on neutrophil-lymphocyte ratio in the hyperglycemic Saudi population. *Medicina (Kaunas)* 2022;**58**:1040. https://doi.org/10.3390/medicina58081040

18. Woo SJ, Ahn SJ, Ahn J, Park KH, Lee K. Elevated systemic neutrophil count in diabetic retinopathy and diabetes: a hospital-based cross-sectional study of 30,793 Korean subjects. *Invest Ophthalmol Vis Sci* 2011;**52**:7697–7703. https://doi.org/10.1167/iovs.11-7784
19. Libby P. Inflammation in atherosclerosis. *Nature* 2002;**420**:868–874. https://doi.org/10.1038/nature01323
20. Toth M, Sohail A, Fridman R. Assessment of gelatinases (MMP-2 and MMP-9) by gelatin zymography. *Methods Mol Biol* 2012;**878**:121–135. https://doi.org/10.1007/978-1-61779-854-2_8
21. Moulding DA, Hart CA, Edwards SW. Regulation of neutrophil Fc gamma RIIIb (CD16) surface expression following delayed apoptosis in response to GM-CSF and sodium butyrate. *J Leukoc Biol* 1999;**65**:875–882. https://doi.org/10.1002/jlb.65.6.875
22. Niven DJ, Berthiaume LR, Fick GH, Laupland KB. Matched case-control studies: a review of reported statistical methodology. *Clin Epidemiol* 2012;**4**:99–110. https://doi.org/10.2147/CLEP.S30816
23. Breslow NE, Day NE. Statistical methods in cancer research. Volume I—the analysis of case-control studies. *IARC Sci Publ* 1980;**32**:5.
24. Faraone SV. Interpreting estimates of treatment effects: implications for managed care. *P T* 2008;**33**:700–711.
25. Cohen J. *Statistical Power Analysis for the Behavioral-Sciences Perceptual and Motor Skills*: Lawrence Erlbaum Associates; 1988. p1007–1007.
26. Xing L, Yamamoto E, Sugiyama T, Jia HB, Ma LJ, Hu SN, *et al.* EROSION Study (effective anti-thrombotic therapy without stenting: intravascular optical coherence tomography-based management in plaque erosion) a 1-year follow-up report. *Circ Cardiovasc Interv* 2017;**10**:e005860. https://doi.org/10.1161/CIRCINTERVENTIONS.117.005860
27. Libby P, Pasterkamp G. Requiem for the 'vulnerable plaque'. *Eur Heart J* 2015;**36**:2984–2987. https://doi.org/10.1093/eurheartj/ehv349
28. Iyer RP, Jung M, Lindsey ML. MMP-9 signaling in the left ventricle following myocardial infarction. *Am J Physiol Heart Circ Physiol* 2016;**311**:H190–H198. https://doi.org/10.1152/ajpheart.00243.2016
29. Lindsey M, Wedin K, Brown MD, Keller C, Evans AJ, Smolen J, *et al.* Matrix-dependent mechanism of neutrophil-mediated release and activation of matrix metalloproteinase 9 in myocardial ischernia/reperfusion. *Circulation* 2001;**103**:2181–2187. https://doi.org/10.1161/01.CIR.103.17.2181
30. Hemdahl AL, Gabrielsen A, Zhu CY, Eriksson P, Hedin U, Kastrup J, *et al.* Expression of neutrophil gelatinase-associated lipocalin in atherosclerosis and myocardial infarction. *Arterioscler Thromb Vasc Biol* 2006;**26**:136–142. https://doi.org/10.1161/01.ATV.0000193567.88685.f4
31. Wang Y, Wu JM, Newton R, Bahaie NS, Long CM, Walcheck B. ADAM17 Cleaves CD16b (Fc gamma RIIIb) in human neutrophils. *Biochim Biophys Acta* 2013;**1833**:680–685. https://doi.org/10.1016/j.bbamcr.2012.11.027
32. Dransfield I, Buckle AM, Savill JS, Mcdowall A, Haslett C, Hogg N. Neutrophil apoptosis is associated with a reduction in Cd16 (Fc-Gamma-Riii) expression. *J Immunol* 1994;**153**:1254–1263. https://doi.org/10.4049/jimmunol.153.3.1254
33. Scheibner KA, Lutz MA, Boodoo S, Fenton MJ, Powell JD, Horton MR. Hyaluronan fragments act as an endogenous danger signal by engaging TLR2. *J Immunol* 2006;**177**:1272–1281. https://doi.org/10.4049/jimmunol.177.2.1272
34. Libby P. Mechanisms of acute coronary syndromes. *N Engl J Med* 2013;**369**:883–884. https://doi.org/10.1056/NEJMc1307806
35. Jang IK, Tearney GJ, MacNeill B, Takano M, Moselewski F, Iftima N, *et al.* In vivo characterization of coronary atherosclerotic plaque by use of optical coherence tomography. *Circulation* 2005;**111**:1551–1555. https://doi.org/10.1161/01.CIR.0000159354.43778.69
36. Naruko T, Ueda M, Haze K, van der Wal AC, van der Loos CM, Itoh A, *et al.* Neutrophil infiltration of culprit lesions in acute coronary syndromes. *Circulation* 2002;**106**:2894–2900. https://doi.org/10.1161/01.CIR.0000042674.89762.20
37. Ji ZJ, Liu GR, Guo JQ, Zhang R, Su YM, Carvalho A, *et al.* The neutrophil-to-lymphocyte ratio is an important indicator predicting in-hospital death in AMI patients. *Front Cardiovasc Med* 2021;**8**:706852. https://doi.org/10.3389/fcvm.2021.706852
38. Curtiss LK, Tobias PS. Emerging role of Toll-like receptors in atherosclerosis. *J Lipid Res* 2009;**50**:S340–S345. https://doi.org/10.1194/jlr.R800056-JLR200
39. Pedicino D, Vinci R, Giglio AF, Pisano E, Porto I, Vergallo R, *et al.* Alterations of hyaluronan metabolism in acute coronary syndrome. *J Am Coll Cardiol* 2018;**72**:1490–1503. https://doi.org/10.1016/j.jacc.2018.06.072
40. Kolodgie FD, Burke AP, Farb A, Weber DK, Kutys R, Wight TN, *et al.* Differential accumulation of proteoglycans and hyaluronan in culprit lesions: insights into plaque erosion. *Arterioscler Thromb Vasc Biol* 2002;**22**:1642–1648. https://doi.org/10.1161/01.ATV.0000034021.92658.4C
41. Quero L, Klawitter M, Schmaus A, Rothley M, Sleeman J, Tiaden AN, *et al.* Hyaluronic acid fragments enhance the inflammatory and catabolic response in human intervertebral disc cells through modulation of toll-like receptor 2 signalling pathways. *Arthritis Res Ther* 2013;**15**:R94. https://doi.org/10.1186/ar4274
42. Vinci R, Pedicino D, D'Aiello A, Ciampi P, Ponzo M, Bonanni A, *et al.* Platelet hyaluronidase 2 enrichment in acute coronary syndromes: a conceivable role in monocyte-platelet aggregate formation. *J Enzyme Inhib Med Chem* 2021;**36**:785–789. https://doi.org/10.1080/14756366.2021.1900159
43. Lepperdinger G, Strobl B, Kreil G. HYAL2, a human gene expressed in many cells, encodes a lysosomal hyaluronidase with a novel type of specificity. *J Biol Chem* 1998;**273**:22466–22470. https://doi.org/10.1074/jbc.273.35.22466
44. Shah PK, Galis ZS. Matrix metalloproteinase hypothesis of plaque rupture—players keep piling up but questions remain. *Circulation* 2001;**104**:1878–1880. https://doi.org/10.1161/circ.104.16.1878
45. Li T, Li X, Feng Y, Dong G, Wang Y, Yang J. The role of matrix metalloproteinase-9 in atherosclerotic plaque instability. *Mediators Inflamm* 2020;**2020**:3872367. https://doi.org/10.1155/2020/3872367
46. Brown DL, Hibbs MS, Kearney M, Loushin C, Isner JM. Identification of 92-kD gelatinase in human coronary atherosclerotic lesions. Association of active enzyme synthesis with unstable angina. *Circulation* 1995;**91**:2125–2131. https://doi.org/10.1161/01.CIR.91.8.2125
47. Newby AC. Dual role of matrix metalloproteinases (matrixins) in intimal thickening and atherosclerotic plaque rupture. *Physiol Rev* 2005;**85**:1–31. https://doi.org/10.1152/physrev.00048.2003
48. Shah PK. Mechanisms of plaque vulnerability and rupture. *J Am Coll Cardiol* 2003;**41**:15s–22s. https://doi.org/10.1016/S0735-1097(02)02834-6
49. Bentzon JF, Otsuka F, Virmani R, Falk E. Mechanisms of plaque formation and rupture. *Circ Res* 2014;**114**:1852–1866. https://doi.org/10.1161/CIRCRESAHA.114.302721
50. Laronha H, Caldeira J. Structure and function of human matrix metalloproteinases. *Cells* 2020;**9**:1076. https://doi.org/10.3390/cells9051076
51. Halade GV, Jin YF, Lindsey ML. Matrix metalloproteinase (MMP)-9: a proximal biomarker for cardiac remodeling and a distal biomarker for inflammation. *Pharmacol Ther* 2013;**139**:32–40. https://doi.org/10.1016/j.pharmthera.2013.03.009
52. Ardi VC, Kupriyanova TA, Deryugina EI, Quigley JP. Human neutrophils uniquely release TIMP-free MMP-9 to provide a potent catalytic stimulator of angiogenesis. *Proc Natl Acad Sci U S A* 2007;**104**:20262–20267. https://doi.org/10.1073/pnas.0706438104
53. Bradley LM, Douglass MF, Chatterjee D, Akira S, Baaten BJ. Matrix metalloprotease 9 mediates neutrophil migration into the airways in response to influenza virus-induced toll-like receptor signaling. *PLoS Pathog* 2012;**8**:e1002641. https://doi.org/10.1371/journal.ppat.1002641
54. Kelly D, Cockerill G, Ng LL, Thompson M, Khan S, Samani NJ, *et al.* Plasma matrix metalloproteinase-9 and left ventricular remodelling after acute myocardial infarction in man: a prospective cohort study. *Eur Heart J* 2007;**28**:711–718. https://doi.org/10.1093/eurheartj/ehm003
55. Angelini G, Flego D, Vinci R, Pedicino D, Trotta F, Ruggio A, *et al.* Matrix metalloproteinase-9 might affect adaptive immunity in non-ST segment elevation acute coronary syndromes by increasing CD31 cleavage on CD4+ T-cells. *Eur Heart J* 2018;**39**:1089–1097. https://doi.org/10.1093/eurheartj/ehx684
56. Gupta AK, Joshi MB, Philippova M, Erne P, Hasler P, Hahn S, *et al.* Activated endothelial cells induce neutrophil extracellular traps and are susceptible to NETosis-mediated cell death. *FEBS Lett* 2010;**584**:3193–3197. https://doi.org/10.1016/j.febslet.2010.06.006
57. Saffarzadeh M, Juenemann C, Queisser MA, Lochnit G, Barreto G, Galuska SP, *et al.* Neutrophil extracellular traps directly induce epithelial and endothelial cell death: a predominant role of histones. *PLoS One* 2012;**7**:e32366. https://doi.org/10.1371/journal.pone.0032366
58. Rosales C. Neutrophil: a cell with many roles in inflammation or several cell types? *Front Physiol* 2018;**9**:113. https://doi.org/10.3389/fphys.2018.00113
59. Souto FO, Alves-Filho JC, Turato WM, Auxiliadora-Martins M, Basile-Filho A, Cunha FQ. Essential role of CCR2 in neutrophil tissue infiltration and multiple organ dysfunction in sepsis. *Am J Respir Crit Care Med* 2011;**183**:234–242. https://doi.org/10.1164/rccm.201003-0416OC
60. Sonego F, Castanheira FV, Ferreira RG, Kanashiro A, Leite CA, Nascimento DC, *et al.* Paradoxical roles of the neutrophil in sepsis: protective and deleterious. *Front Immunol* 2016;**7**:155. https://doi.org/10.3389/fimmu.2016.00155
61. Lima CX, Souza DG, Amaral FA, Fagundes CT, Rodrigues IP, Alves-Filho JC, *et al.* Therapeutic effects of treatment with anti-TLR2 and anti-TLR4 monoclonal antibodies in polymicrobial sepsis. *PLoS One* 2015;**10**:e0132336. https://doi.org/10.1371/journal.pone.0132336
62. Ziegler G, Freyer D, Harhausen D, Khojasteh U, Nietfeld W, Trendelenburg G. Blocking TLR2 in vivo protects against accumulation of inflammatory cells and neuronal injury in experimental stroke. *J Cereb Blood Flow Metab* 2011;**31**:757–766. https://doi.org/10.1038/jcbfm.2010.161
63. Wang L, Li YL, Zhang CC, Cui W, Wang X, Xia Y, *et al.* Inhibition of Toll-like receptor 2 reduces cardiac fibrosis by attenuating macrophage-mediated inflammation. *Cardiovasc Res* 2014;**101**:383–392. https://doi.org/10.1093/cvr/cvt258
64. Arslan F, Houtgraaf JH, Keogh B, Kazemi K, de Jong R, McCormack WJ, *et al.* Treatment with OPN-305, a humanized anti-Toll-like receptor-2 antibody, reduces myocardial ischemia/reperfusion injury in pigs. *Circ Cardiovasc Interv* 2012;**5**:279–287. https://doi.org/10.1161/CIRCINTERVENTIONS.111.967596
65. Ding J, Liang TXZ, Zhou Y, He ZW, Min QH, Jiang LP, *et al.* Hyaluronidase-triggered anticancer drug and siRNA delivery from cascaded targeting nanoparticles for drug-resistant breast cancer therapy. *Nano Res* 2017;**10**:690–703. https://doi.org/10.1007/s12274-016-1328-y
66. Anwar MA, Shah M, Kim J, Choi S. Recent clinical trends in Toll-like receptor targeting therapeutics. *Med Res Rev* 2019;**39**:1053–1090. https://doi.org/10.1002/med.21553

67. Farhat K, Riekenberg S, Heine H, Debarry J, Lang R, Mages J, *et al.* Heterodimerization of TLR2 with TLR1 or TLR6 expands the ligand spectrum but does not lead to differential signaling. *J Leukoc Biol* 2008;**83**:692–701. https://doi.org/10.1189/jlb.0807586
68. Long EM, Millen B, Kubes P, Robbins SM. Lipoteichoic acid induces unique inflammatory responses when compared to other Toll-like receptor 2 ligands. *PLoS One* 2009;**4**: e5601. https://doi.org/10.1371/journal.pone.0005601
69. Cyphert JM, Trempus CS, Garantziotis S. Size matters: molecular weight specificity of hyaluronan effects in cell biology. *Int J Cell Biol* 2015;**2015**:563818. https://doi.org/10.1155/2015/563818
70. Laurent UBG, Tengblad A. Determination of hyaluronate in biological samples by a specific radioassay technique. *Anal Biochem* 1980;**109**:386–394. https://doi.org/10.1016/0003-2697(80)90665-X
71. Chichibu K, Matsuura T, Shichijo S, Yokoyama MM. Assay of serum hyaluronic-acid in clinical-application. *Clin Chim Acta* 1989;**181**:317–323. https://doi.org/10.1016/0009-8981(89)90237-4
72. Cowman MK, Lee HG, Schwertfeger KL, McCarthy JB, Turley EA. The content and size of hyaluronan in biological fluids and tissues. *Front Immunol* 2015;**6**:261. https://doi.org/10.3389/fimmu.2015.00261
73. Fraser JRE, Laurent TC, Laurent UBG. Hyaluronan: its nature, distribution, functions and turnover. *J Intern Med* 1997;**242**:27–33. https://doi.org/10.1046/j.1365-2796.1997.00170.x
74. Kuehl C, Zhang T, Kaminskas LM, Porter CJH, Davies NM, Forrest L, *et al.* Hyaluronic acid molecular weight determines lung clearance and biodistribution after instillation. *Mol Pharm* 2016;**13**:1904–1914. https://doi.org/10.1021/acs.molpharmaceut.6b00069

Curriculum Vitae

Mein Lebenslauf wird aus datenschutzrechtlichen Gründen in der elektronischen Version meiner Arbeit nicht veröffentlicht.

List of Publications

1: Nelles G, Abdelwahed YS, Seppelt C, **Meteva D**, Stähli BE, Rai H, Seegers LM, Sieronski L, Musfeldt J, Gerhardt T, Riedel M, Skurk C, Haghikia A, Sinning D, Dreger H, Knebel F, Trippel TD, Krisper M, Klotsche J, Joner M, Landmesser U, Leistner DM. *Cholesterol crystals at the culprit lesion in patients with acute coronary syndrome are associated with worse cardiovascular outcomes at two years follow up - results from the translational OPTICO-ACS study program*. Int J Cardiol. 2023 Dec 22:131665. doi: 10.1016/j.ijcard.2023.131665. Epub ahead ofprint. PMID: 38141724.

2: Nelles G, Abdelwahed YS, Alyaqoob A, Seppelt C, Stähli BE, **Meteva D**, Kränkel N, Haghikia A, Skurk C, Dreger H, Knebel F, Trippel TD, Krisper M, Sieronski L, Gerhardt T, Zanders L, Klotsche J, Landmesser U, Joner M, Leistner DM. *Spotty calcium deposits within acute coronary syndrome (ACS)-causing culprit lesions impact inflammatory vessel-wall interactions and are associated with higher cardiovascular event rates at one year follow-up: Results from the prospective translational OPTICO-ACS study program*. Atherosclerosis. 2023 Nov;385:117284. doi: 10.1016/j.atherosclerosis.2023.117284. Epub 2023 Sep 15. PMID: 37871405.

3: Seppelt C, Abdelwahed YS, **Meteva D**, Nelles G, Stähli BE, Erbay A, Kränkel N, Sieronski L, Skurk C, Haghikia A, Sinning D, Dreger H, Knebel F, Trippel TD, Krisper M, Gerhardt T, Rai H, Klotsche J, Joner M, Landmesser U, Leistner DM. *Coronary microevaginations characterize culprit plaques and their inflammatory microenvironment in a subtype of acute coronary syndrome with intact fibrous cap: results from the prospective translational OPTICO-ACS study.* Eur Heart J Cardiovasc Imaging. 2024 Jan 29;25(2):175-184. doi: 10.1093/ehjci/jead154. PMID: 37395586.

4: Cuadrat RRC, Kratzer A, Arnal HG, Rathgeber AC, Wreczycka K, Blume A, Gündüz IB, Ebenal V, Mauno T, Osberg B, Moobed M, Hartung J, Jakobs K, Seppelt C, **Meteva D**, Haghikia A, Leistner DM, Landmesser U, Akalin A. *Cardiovascular disease biomarkers derived from circulating cell-free DNA methylation*. NAR Genom Bioinform. 2023 Jun 28;5(2):lqad061. doi: 10.1093/nargab/lqad061. PMID: 37388821; PMCID: PMC10304763.

5: Gerhardt T, Seppelt C, Abdelwahed YS, **Meteva D**, Wolfram C, Stapmanns P, Erbay A, Zanders L, Nelles G, Musfeld J, Sieronski L, Stähli BE, Montone RA, Vergallo R,

Haghikia A, Skurk C, Knebel F, Dreger H, Trippel TD, Rai H, Joner M, Klotsche J, Libby P, Crea F, Kränkel N, Landmesser U, Leistner DM; OPTICO-ACS study group. *Culprit plaque morphology determines inflammatory risk and clinical outcomes in acute coronary syndrome*. Eur Heart J. 2023 Oct 12;44(38):3911-3925. doi: 10.1093/eurheartj/ehad334. PMID: 37381774.

6: **Meteva D**, Vinci R, Seppelt C, Abdelwahed YS, Pedicino D, Nelles G, Skurk C, Haghikia A, Rauch-Kröhnert U, Gerhardt T, Straessler E, Zhao Y, Golla F, Joner M, Rai H, Kratzer A, Arnal HG, Liuzzo G, Klotsche J, Crea F, Landmesser U, Leistner DM, Kränkel N. *Toll-like receptor 2, hyaluronan, and neutrophils play a key role in plaque erosion: the OPTICO-ACS study*. Eur Heart J. 2023 Oct 12;44(38):3892-3907. doi: 10.1093/eurheartj/ehad379. PMID: 37381760.

7: Giral H, Franke V, Moobed M, Müller MF, Lübking L, James DM, Hartung J, Kuschnerus K, **Meteva D**, Seppelt C, Jakob P, Klingenberg R, Kränkel N, Leistner D, Zeller T, Blankenberg S, Zimmermann F, Haghikia A, Lüscher TF, Akalin A, Landmesser U, Kratzer A. *Rapid Inflammasome Activation Is Attenuated in Post- Myocardial Infarction Monocytes*. Front Immunol. 2022 Apr 26;13:857455. doi: 10.3389/fimmu.2022.857455. PMID: 35558073; PMCID: PMC9090500.

8: Abdelwahed YS, Nelles G, Frick C, Seppelt C, **Meteva D**, Stähli BE, Rai H, Riedel M, Skurk C, Rauch-Kröhnert U, Haghikia A, Sinning D, Dreger H, Knebel F, Trippel T, Krisper M, Klotsche J, Joner M, Landmesser U, Leistner DM. *Coexistence of calcified- and lipid-containing plaque components and their association with incidental rupture points in acute coronary syndrome-causing culprit lesions: results from the prospective OPTICO-ACS study*. Eur Heart J Cardiovasc Imaging. 2022 Nov 17;23(12):1598-1605. doi: 10.1093/ehjci/jeab247. PMID: 34904655.

9: Seppelt C, Abdelwahed YS, **Meteva D**, Leistner DM. *Intrakoronare Bildgebung – wie die Plaque-Morphologie die Therapie personalisiert [Intracoronary imaging - how plaque morphology impacts personal medical therapy].* Dtsch Med Wochenschr. 2021 Nov;146(23):1547-1551. German. doi: 10.1055/a-1361-8103. Epub 2021 Nov 26. PMID: 34826842.

10: **Meteva D**, Seppelt C, Abdelwahed YS, Leistner DM. *Distinct pathological mechanisms distinguish acute coronary syndrome caused by plaque erosion from plaque rupture*. Curr Opin Cardiol. 2021 Nov 1;36(6):793-797. doi: 10.1097/HCO.0000000000000912. PMID: 34620794.

11: Reinthaler M, Grosshauser J, Schmidt T, Unger J, Morgan R, Zimmermann F, Hartung J, Seppelt C, **Meteva D**, Haider W, Landmesser U, Skurk C. *Preclinical assessment of a modified Occlutech left atrial appendage closure device in a porcine model*. Sci Rep. 2021 Feb 4;11(1):2988. doi: 10.1038/s41598-021-82359-1. PMID: 33542297; PMCID: PMC7862256.

12: Leistner DM, Kränkel N, **Meteva D**, Abdelwahed YS, Seppelt C, Stähli BE, Rai H, Skurk C, Lauten A, Mochmann HC, Fröhlich G, Rauch-Kröhnert U, Flores E, Riedel M, Sieronski L, Kia S, Strässler E, Haghikia A, Dirks F, Steiner JK, Mueller DN, Volk HD, Klotsche J, Joner M, Libby P, Landmesser U. *Differential immunological signature at the culprit site distinguishes acute coronary syndrome with intact from acute coronary syndrome with ruptured fibrous cap: results from the prospective translational OPTICO-ACS study*. Eur Heart J. 2020 Oct 1;41(37):3549-3560. doi: 10.1093/eurheartj/ehaa703. PMID: 33080003; PMCID: PMC7780480.

Acknowledgements

My deepest acknowledgements for the professional assistance and scientific guidance go to my supervisors: PD. Dr. N. Kränkel and Prof. Dr. D. Leistner as well as to my mother for her emotional support and encouragement